

Theory of Resistive and Ideal Internal Kinks

RLE Technical Report No. 568

Stefano Migliuolo

February 1992

**Research Laboratory of Electronics
Massachusetts Institute of Technology
Cambridge, Massachusetts 02139-4307**

This work was supported in part by the U.S. Department of Energy under Contract DE-FG02-91ER-54109.

THEORY OF RESISTIVE AND IDEAL INTERNAL KINKS

S. Migliuolo

Massachusetts Institute of Technology
Research Laboratory of Electronics

Abstract

A review of the present theoretical understanding of the linear stability of internal $m^0 = 1$ modes is presented and its connection to phenomena observed in toroidal magnetic confinement experiments, i.e. "sawtooth" and "fishbone" oscillations, is discussed. Particular attention is devoted to the analysis of non-magnetohydrodynamic (MHD) effects, such as those due to finite diamagnetic and electron drift frequencies and ion Larmor radius, and to the special role played by energetic particles (whose response is wholly kinetic and which can stabilize these modes).

I. Introduction

The initial discovery [1] of so-called “sawtooth” oscillations in toroidal experiments indicated the presence of a cyclical process in which the steady rise in intensity of x-rays emitted from the center of the plasma was interrupted by a sudden drop in this emission, indicating either a rapid cooling of the plasma center or an expulsion of the hot core. Following initial work on ideal magnetohydrodynamic (MHD) instabilities [2] in which the existence and accessibility of neighboring equilibria were proved, and in which it was shown that these unstable modes would be too weak to explain the experiment, Kadomtsev proposed a complete reconnection model [3] in which a resistive $m^0 = n^0 = 1$ instability displaces the center region of the plasma (defined as the region within which the magnetic winding index, $q(r) = rB_\zeta/RB_\theta$ falls below unity; B_ζ and B_θ are the toroidal and poloidal components of the magnetic field, respectively) leading to the crowding of flux surfaces on one side, the creation of a magnetic X-point, and the eventual breaking and reconnection of magnetic field lines. An intermediate state exists in this picture, consisting of a displaced, though still circular, hot core and a cool island partially surrounding it. It is followed by the expulsion of the core and re-circularization of the flux surfaces. In his model, Kadomtsev gave an estimate for the time required for complete reconnection, $\tau \sim \sqrt{\pi\sigma r_s^2 R/c^2 V_A}$, and a diagrammatical prescription for determining the radial profile of the reconnected flux, given the initial profile $\psi_0(r)$. Above, we denoted by $V_A = B_\zeta/\sqrt{4\pi n m_i}$ the Alfvén speed, r_s the radius of the singular surface where $q(r) = 1$, R the major radius, while $\sigma = 1/\eta$ is the parallel electrical conductivity. While providing a plausible scenario of the sawtooth crash, Kadomtsev’s model could at best only give order of magnitude estimates

for the relevant time scales.

The first derivation of the linear growth time for resistive $m^0 = 1$ instabilities, $\tau_R \sim \tau_H \epsilon_\eta^{-1/3}$ where $\tau_H = \sqrt{3}R/V_A$ is the hydrodynamic time and $\epsilon_\eta = \eta c^2 \tau_H / 4\pi r_s^2$, was given by Coppi *et al.* [4]. Later [5] they showed how finite ion diamagnetic frequency, ω_{di} , effects could further increase this characteristic time: $\tau_{R*} \sim \omega_{di}^2 \tau_H^3 \epsilon_\eta^{-1}$. Much experimental evidence has accumulated since these early papers, indicating that the sawtooth crash involves both the central electron temperature (inferred from electron cyclotron emission, ECE, interferometry) and the electron density (inferred from millimeter-range wave scattering measurements), as shown for instance on JET by Campbell *et al.* [6]. When the pre-crash density profile is rather flat, as happens in Doublet-III, the sawtooth is detectable also in the electron density, though it has much smaller amplitude than that in the temperature [7]. The detection of density crashes gives preference to models (including Kadomtsev's) in which the physics of the sawtooth culminates with the expulsion of the central plasma core.

With the advent of large high temperature experiments with sophisticated X-ray tomography, new evidence has come to light, which casts doubts on the applicability of models that depend exclusively on resistive reconnection to produce the sawtooth. The first critical piece of evidence involves the relevant time scale: in JET [8] the central plasma core is initially displaced sideways and then redistributed poloidally in a very short time scale, $\tau \approx 100\text{--}200 \mu\text{sec}$. While the initial motion is consistent with an $m^0 = n^0 = 1$ perturbation, the time scale is much shorter than the simple resistive time, $\tau_R \sim 400 \mu\text{sec}$, and an order of magnitude smaller than the growth time predicted when diamagnetic effects

are included, $\tau_{R*} \sim 10\text{--}30$ msec. This latter time is predicted by linear theory [5] to be the relevant time for instability. Note that the observed time is commensurate with the linear growth time of an ideal instability, $\tau_I \sim C_0(R/r_s)^2\tau_H$ (where we assumed that $r_s \approx \sqrt{ab}/3$, a and b being the horizontal and vertical minor radii, respectively), provided the constant $1/C_0$ which represents how far the plasma is above threshold, is assigned the value 0.1. There exist measurements in at least two experiments that indicate that the threshold for ideal-MHD instability may indeed have been surpassed. In neutral beam heated experiments on Doublet-III [7], giant sawteeth with inversion radii $r/a = 0.4\text{--}0.5$ were observed in conjunction with poloidal beta, $\beta_p^{exp} = 8\pi \langle\langle p \rangle\rangle / B_\theta^2(r = a)$, reaching values of 0.7. In the experiment JIPP T-II, both Ohmic and neutral beam heated plasmas were found [9] to achieve values $\beta_p = 0.6\text{--}0.7$, where now $\beta_p \equiv [-8\pi/B_\theta^2(r = r_s)] \int_0^{r_s} dr (r/r_s)^2 (dP/dr)$ is computed in the manner appropriate for comparison with theory [10]. If we adopt the quantity $\lambda_H = (3\pi/2)(r_s/R)^2[\beta_p^2 - \beta_{pc}^2]$ as the parameter relevant to ideal instability, estimate $\beta_{pc} \approx 0.25$, $r_s = a/3$, and $r_p = -(d \ln P/dr)^{-1} = a/2$, we obtain: $\lambda_H \approx 5 \cdot 10^{-3} \geq \omega_{di}\tau_H/2$. This tells us that the experiment on JIPP T-II operated at a value of β_p that was sufficient to overcome the FLR stabilization of the ideal $m^0 = 1$ instability, since the dispersion relation for ideal modes is [5]: $\omega^2 - \omega\omega_{di} + \lambda_H^2/\tau_H^2 = 0$.

A second critique of the complete reconnection model comes from the topology of the island, inferred from both soft X-ray tomography and ECE diagnostics. Both Edwards *et al.* [8] and Westerhof *et al.* [11] conclude that, in JET, a complete sawtooth collapse involves a stage in which a displaced hot core has deformed into an island that partially surrounds a new cold core. This is in complete contradiction with the picture presented by

Kadomtsev [3] as discussed at the beginning of this section. Note that Westerhof *et al.* [11] as well as Campbell *et al.* [12] mention the possibility that, while Kadomtsev's complete reconnection model appears to fail for full sawtooth crashes in JET, it may correctly apply to partial sawteeth for which the magnetic topology indicates a cold island (cf. Figs. 1 and 2 in Ref. [11]). For partial sawteeth, a "crash" time is difficult to obtain from the time trace of the signal (e.g., Fig. 1(a) of Ref. [11] and Fig. 3 of Ref. [12]). Often, in these cases, the amplitude of the successor oscillation is initially as large as the crash itself. There is evidence [12] that partial sawtooth collapses actually form a spectrum of phenomena whose characteristic time can be very rapid ("fast" partial sawteeth) or much slower ("slow" partial sawteeth), while full sawtooth collapses are always fast (e.g., Fig. 1 of Ref. [12]). The two main differences between full and partial sawteeth, apart from (possibly) island topology and time constants, are the amplitude of the successor oscillation relative to the size of the crash (the ratio is much smaller for full sawteeth than for partial sawteeth) and the return of the hot core to its initial central position in the case of partial sawteeth (in the case of a full collapse, the deformed hot core flows in the poloidal direction and establishes a ring of warm plasma). The topology of the deformed magnetic surfaces is, at the time of this writing, an unresolved issue. Contrary to the JET results, experiments in TFTR [13]-[14] seem to indicate the presence of a displaced hot circular core, surrounded by a crescent shaped cold island, in most cases. Thus, one is tempted to attribute the observed difference in topology of the reconnection process to experimental factors, such as circular vs. "D"-shaped equilibrium flux surfaces [J. F. Drake, private communication, 1990]. Until an experimental campaign of careful comparison between

the two experiments is conducted and/or a statistical data base of island topologies is assembled, this question will likely remain unanswered.

One last detail worth discussing is the role played by finite diamagnetic frequency effects. From our expressions for τ_R and τ_{R*} and the corresponding estimates for the JET experiment, it is obvious that the presence of ω_{di} is a major cause for discrepancy between theoretical predictions and the observations. Since $\omega_{di} \propto dP/dr$ and the sawtooth collapse is likely to flatten the pressure profile inside the $q(r) = 1$ surface, one is led to believe that finite- ω_{di} must act as a barrier against the initial trigger for the crash, though not necessarily influencing the crash itself (e.g., fast nonlinear growth once the threshold for instability is surpassed [15]). There exists at least partial evidence of this barrier from ASDEX [16] and JT-60 [17] where a strongly peaked electron density profile (due to pellet injection) was seen to suppress sawteeth and/or lengthen the period between sawteeth by an order of magnitude. Also, a series of reconstructed soft X-ray profiles in the Tokamak de Varennes [18] over a time span $\Delta t \approx 0.1$ sec clearly shows the rotation (in the poloidal direction) of the hot core, suggestive of diamagnetic or $\mathbf{E} \times \mathbf{B}$ rotation. Extremely clear examples of precursor oscillations in JET (cf. Fig. 4 of Ref. [6]) are the most direct evidence of finite ω_{di} , while the presence of strong “postcursor” oscillations after partial sawtooth collapses [12] indicates that the pressure profile within the $q(r) = 1$ surface is not always completely flattened.

In this work, we consider the status of our present theoretical understanding of sawtooth oscillations, within the context of the linear instability of an $m^0 = n^0 = 1$ perturbation (so-called “internal kink”). Such an oscillation has been detected, at times [6],

preceding the crash itself; hence the name “precursor oscillation”. We will mostly confine ourselves to cases where the magnetic shear is finite; this is the situation that has been studied the most. Some remarks on low or zero shear models are made in the conclusions. In Sec. II we review the basic theory which employs the two-fluid equations of Braginskii and which is applicable to low temperature Ohmic experiments. The different roles played by electrical resistivity, ion diamagnetic frequency and collisional viscosity, and electron drift wave frequency are pointed out and the principal method of solution (involving generalized Fourier transforms) is described. Extension of the fluid theory to low-collisionality regimes, where finite electron inertia becomes a dominant contribution to Ohm’s law, is also discussed. The generalization of the theory to kinetic regimes is detailed in Sec. III where finite ion Larmor radius (FLR) and electron kinetic effects are considered; these regimes are reached, e.g., in high temperature experiments in large machines with relatively low density, such as JET and TFTR. The consequences of having an energetic species of particles in the plasma are discussed in Sec. IV. Among those are the stabilization of the ideal and resistive internal kinks (sawtooth-free regimes which were first termed “monster sawteeth”) and the production of so-called “fishbone oscillation bursts”. Our conclusions and discussion of open questions follows in Sec. V.

II. Fluid Theory

II.1 General considerations

If one considers a current carrying plasma in the cylindrical approximation where

$$\mathbf{B} = B_z(r)\hat{e}_z + B_\theta(r)\hat{e}_\theta \quad (\text{II.1})$$

and computes the change in potential energy due to an ideal-MHD perturbation, one finds (see, e.g., [19]):

$$\delta W = \frac{\pi}{2} \int_0^a \left[f(r) \left(\frac{d\xi}{dr} \right)^2 + g(r) \xi^2(r) \right] \quad (\text{II.2})$$

where ξ is the radial component of the Lagrangian displacement; a minimization with respect to the other two components has already been carried out, yielding conditions for incompressibility ($\nabla \cdot \vec{\xi} = 0$) and decoupling the perturbation from the fast magnetosonic mode. The expressions for the two quantities, f and g are (for the special case where $\xi \sim \exp(i\theta - iz/R)$):

$$f(r) = \frac{r^3 F^2}{1 + r^2/R^2} \quad (\text{II.3})$$

$$g(r) = \frac{r^2/R^2}{1 + r^2/R^2} \left[8\pi \frac{dP}{dr} + rF^2 + 2 \frac{rB_z^2/R^2}{1 + r^2/R^2} \left(1 - \frac{1}{q^2} \right) \right] \quad (\text{II.4})$$

where we defined $q(r) = rB_z/RB_\theta$ (the cylindrical equivalent of the magnetic winding index defined in the introduction) and $F = \mathbf{k} \cdot \mathbf{B} = -B_z/R + B_\theta/r$. The first term within g represents the contribution of the pressure gradient to interchange-type modes, the second is the bending of the magnetic field lines (a stabilizing effect), while the third drives the internal kink unstable in a zero- β plasma when $q(r) < 1$. The important point, here, is that $g(r)$ is of order $\epsilon^2 F^2$ where $\epsilon \equiv r/R$ and, thus, toroidal effects (themselves of order ϵ^2) will play an important role. The change in potential energy in toroidal geometry has

been computed, e.g. in [10], [20], where it was shown that the instability requires pressure gradients in excess of a critical value (cf. our expression for λ_H in the introduction) that is largely dependent on magnetic shear.

Since $g(r) \sim \epsilon^2 F^2$ while $f(r) \sim F^2$, it becomes obvious that the displacement which minimizes the change in potential energy (and is therefore favored from an energetic standpoint) to order ϵ , is one with zero derivative in r everywhere except at $r = r_s$ where $F(r)$ vanishes. Thus the solution is constructed [5] as follows:

$$\xi = \xi_0 + \epsilon^2 \xi_2(r) \quad (\text{II.5})$$

where, in the region $r \leq r_s$

$$\xi_0 = \xi_\infty = \text{const.}; \quad \frac{d\xi_2}{dr} = \frac{\delta W_{\min}(r)}{\xi_\infty r^3 F^2 \epsilon^2} \quad (\text{II.6})$$

while, in the region $r \geq r_s$

$$\xi_0 = 0; \quad \frac{d\xi_2}{dr} = \frac{\delta W_{\min}(r = r_s)}{\xi_\infty r^3 F^2 \epsilon^2} \quad (\text{II.7})$$

Near $r = r_s$, we have $F(x \equiv (r - r_s)/r_s) \propto x$ and the solution in the ideal-MHD region can be written as:

$$\xi(r) = \xi_\infty H(-x) + \frac{\lambda_H}{\pi x} \quad (\text{II.8})$$

where H is the Heavyside step function and

$$\lambda_H = -\frac{\pi \delta W_{\min}(r = r_s)}{[\xi_\infty B_\theta r dq/dr]_{r_s}^2} \quad (\text{II.9})$$

This solution is actually valid only for $|x| \geq \Delta > 0$, and one must match it to the solution within the inner layer, $|x| \leq \Delta$, which is non-singular. This solution is provided by a

more complete formalism, e.g., the two-fluid resistive description of Braginskii [21], which we consider in the remainder of this section. Note that, at this point the solution in the ideal region becomes the “driver” for the unstable mode (represented by λ_H) through the matching condition.

We refer the reader to Ref. [5] for an original statement of the problem; here we simply sketch the derivation. Within the inner layer, one can neglect toroidal effects. However, inertia, electrical resistivity, and other non-MHD effects are important. Considering a cylindrical geometry for this layer, the plasma equation of motion reads:

$$\rho \left[\frac{\partial \mathbf{V}_i}{\partial t} + (\mathbf{V}_i \cdot \nabla) \mathbf{V}_i \right] = -\nabla p - \nabla \cdot \hat{\hat{\pi}} + \frac{1}{c} \mathbf{J} \times \mathbf{B} \quad (\text{II.10})$$

where $\rho \approx n_i m_i$ is the mass density, $p = p_e + p_i = n(T_e + T_i)$ is the pressure, $\hat{\hat{\pi}}$ is the ion stress tensor, and $\mathbf{J} = en(\mathbf{V}_i - \mathbf{V}_e)$ is the current. Ohm’s law is written as:

$$\begin{aligned} \eta_{\parallel} \mathbf{J}_{\parallel} + \eta_{\perp} \mathbf{J}_{\perp} &= \mathbf{E} + \frac{1}{c} (\mathbf{V}_e \times \mathbf{B}) + \frac{\nabla p_e}{en} \\ &+ \frac{\alpha}{e} \nabla_{\parallel} T_e \end{aligned} \quad (\text{II.11})$$

where the parallel direction is with respect to the magnetic field, $\alpha = 0.71$ is the thermoelectric coefficient of friction (from electron-ion collisions).

The thermal conductivity is assumed low enough so that the temperature evolves through:

$$\frac{3}{2} n \left(\frac{\partial}{\partial t} + \mathbf{V} \cdot \nabla \right) T + p \nabla \cdot \mathbf{V} = 0 \quad (\text{II.12})$$

for electrons and ions.

This set of equations implicitly assumes that the following inequalities hold:

$$\nu_{ei} > \omega; \quad k_{\parallel} V_{Te} / \nu_{ei} < 1; \quad \rho_i / \Delta < 1 \quad (\text{II.13})$$

where $V_{Te} = \sqrt{2T_e/m_e}$ is the electron thermal velocity, ν_{ei} the electron-ion collision frequency, $\rho_i = V_{Ti}/\sqrt{2}\Omega_i$ the ion Larmor radius, and Δ is the thickness of the singular layer. Note that the parallel wavenumber is a function of position, $k_{\parallel}(x) = F/B \approx xs(r_s)/R$ where $s(r) = dq/dr$ is the magnetic shear. The modes of interest will, generally, have frequencies that are significantly lower than the modified electron drift wave frequency, $\hat{\omega}_{*e} = (-n^0 c/enB_{\theta}R)[T_e dn/dr + (1 + \alpha)ndT_e/dr]$. We have consulted published experimental data (for TEXTOR [22], TFTR [23]-[24], and JET [25]-[26]) and obtained the dimensionless ratios shown in Table I. We see that the first inequality is generally satisfied (provided $|\omega| \leq \hat{\omega}_{*e}$), and that the second can be satisfied in the limit of a “thin” singular layer: $|x| \leq \Delta/r_s < \epsilon_{\eta}^{1/3}$ (for all cases except supershots in TFTR [24]). The third inequality requires the situation of a “thick” layer, namely $\Delta > \epsilon_{\eta}^{1/3} r_s$. Since the two trends are in opposite directions, we find that current experiments violate at least one of the last two inequalities shown in (II.13).

The thickness of the layer is controlled by the parameter λ_H in the fluid theory. When $\Delta \sim \lambda_H r_s > \rho_i$, the ions can be treated as a fluid species while the electrons are also fluid but obey an isothermal equation of state (instead of Eq. (II.12)) within most of the singular layer, for the experiments mentioned above. When $\rho_i > \Delta$, the ions must be treated kinetically, while the electrons response can be determined via fluid equations if the layer is thin enough. We will return to this point in the next section.

Here, we review the results obtained from the standard set of equations. Linearizing Eq. (II.10)-(II.12) as well as Maxwell’s equations, and considering the limit $k_z r_s \sim$

$r_s/R \ll 1$, one obtains a set of two coupled differential equations:

$$(\omega - \omega_{di}) \left(\omega - i\nu_\mu \frac{d^2}{dx^2} \right) \frac{d^2 \hat{\xi}}{dx^2} = -\omega_A^2 x \frac{d^2 \psi}{dx^2} \quad (\text{II.14})$$

$$\psi + x \hat{\xi} = i\epsilon_\eta \frac{\omega_A}{\omega - \hat{\omega}_{*e}} \frac{d^2 \psi}{dx^2} \quad (\text{II.15})$$

Here $x = (r - r_s)/r_s$ is the normalized radial variable used previously, $\omega_{di} = (n^0 qc/enB_z r_s)$ $(dp_i/dr)_{r_s}$ is the ion diamagnetic frequency (we took $|k_\theta| = n^0 q/r_s$), $\omega_A = s(r_s)V_A/\sqrt{3}R$ is the Alfvén frequency ($V_A = B_z/\sqrt{4\pi n m_i}$), $\hat{\xi} = \xi(x)/\xi_\infty$ is the normalized radial component of the Lagrangian displacement, and $\psi = i\tilde{B}_r/s(r_s)B_\theta(r_s)$ is the perturbed poloidal magnetic flux. The parallel electrical resistivity appears within $\epsilon_\eta = \eta_{\parallel} c^2/4\pi r_s^2 \omega_A$ (the perpendicular component plays no role), while the ion-ion collisional viscosity appears through $\nu_\mu = \mu_\perp/nm_i r_s^2$ where $\mu_\perp = (3/10)\nu_{ii} n T_i/\Omega_i^2$ is the transverse collisional viscosity [21].

II.2 Limit of negligible ion-ion collisions.

Considering first the limit of vanishing ion viscosity, $\nu_\mu = 0$, an elegant solution of the two coupled second order differential equations (II.14)-(II.15) was originally presented in Ref. [5]. Here we adopt an alternative approach, namely that of first Fourier transforming these equations to conjugate space and then solving the resulting dispersion equation. This method has the advantage of producing a single second order differential equation in the conjugate variable, k (even in the presence of ion collisional viscosity), which is easier to solve than the original set of equations. The concept of a generalized Fourier transform (or, more precisely, the Fourier transform of a “generalized function”, i.e., a function which is not regular but whose integral weighted by an appropriate regular function is finite) was

established long ago [27] and was applied to the stability of low- m^0 modes by Pegoraro and Schep [28]. The Fourier transform of Eq. (II.14)-(II.15) simply is:

$$\begin{aligned} \frac{d}{dk} \left[k^2 \left(1 + i \frac{\epsilon_\eta \omega_A}{\omega - \hat{\omega}_{*e}} k^2 \right)^{-1} \frac{d\xi_k}{dk} \right] \\ + \frac{\omega - \omega_{di}}{\omega_A^2} (\omega + i\nu_\mu k^2) k^2 \xi_k(k) = 0 \end{aligned} \quad (\text{II.16})$$

where ξ_k is the Fourier transform of $\hat{\xi}(x)$. Note that there is no difficulty with the transformation of the resistive equations *per se*; the eigenfunction is regular and a conventional Fourier transform exists. Indeed, the Fourier version of these equations has been known for a long time [29]. The concept of the transform of a generalized function appears through the boundary condition, obtained by matching the inner layer solution to that in the outer (ideal-MHD) layer:

$$\frac{d}{dx} \hat{\xi}(x \rightarrow \infty) = -\frac{\lambda_H \xi_\infty}{\pi x^2} \quad (\text{II.17})$$

which means that $\hat{\xi}(x \rightarrow \infty) \sim 1/x$ and the function “ $1/x$ ” is a generalized function, as defined, e.g., by Gelfand and Shilov [30], whose Fourier transform was written down by Lighthill [27]:

$$\xi_k(k < 1/\delta) = \frac{1}{k} - \lambda_H \text{sgn}(k) \quad (\text{II.18})$$

Note that the transform is defined only for $k^2 > 1$ and, hence, the boundary condition involves ξ_k evaluated for k smaller than the inverse normalized thickness of the singular layer, $1/\delta = \tau_s/\Delta > 1$. The solution of Eq. (II.16), in the limit $\nu_\mu = 0$, is obtained in terms of confluent hypergeometric functions [31]:

$$\xi_k(k) = \xi_{k0} \left[U \left(\frac{Q+1}{4}, \frac{3}{2}, \delta^2 k^2 \right) - \frac{1}{2} \delta^2 k^2 U \left(\frac{Q+5}{4}, \frac{5}{2}, \delta^2 k^2 \right) \right] \exp \left(\frac{1}{2} \delta^2 k^2 \right) \quad (\text{II.19})$$

where

$$\delta \equiv \left(-i\epsilon_\eta \frac{\omega}{\omega_A} \frac{\omega - \omega_{di}}{\omega - \hat{\omega}_{*e}} \right)^{1/4} \quad (\text{II.20})$$

and

$$Q \equiv \left[i \frac{\omega(\omega - \omega_{di})(\omega - \hat{\omega}_{*e})}{\epsilon_\eta \omega_A^3} \right]^{1/2} \quad (\text{II.21})$$

From Eq. (II.19) we see how $1/\delta$ defines the scale in Fourier conjugate space, and, thus, δ is a measure of the thickness of the singular layer. Applying boundary condition (II.18) yields the dispersion relation, first given in Ref. [5]:

$$\left[-\frac{\omega(\omega - \omega_{di})}{\omega_A^2} \right]^{1/2} = \frac{\lambda_H}{8} Q^{3/2} \frac{\Gamma[(Q-1)/4]}{\Gamma[(Q+5)/4]} \quad (\text{II.22})$$

Solutions of this equation can either be obtained numerically or, in various limits, analytically. Examples of some of these limits can be found in Ref. [5] and a pictorial representation of the various regimes of instability (ideal, resistive, tearing,...) has been presented, e.g., in [32]-[34]. In particular, we point out a couple of regimes of importance. First, in the ideal regime, $|Q| \rightarrow \infty$ and Eq. (II.22) yields the well-known solution:

$$\omega = \frac{1}{2}\omega_{di} \pm i\sqrt{\lambda_H^2 \omega_A^2 - \frac{1}{4}\omega_{di}^2} \quad (\text{II.23})$$

Second, in the resistive regime $|Q| \approx 1$ and we find [34]:

$$Q \approx 1 + \frac{2\lambda_H}{\Gamma(1/4)} \left[-\frac{\omega(\omega - \omega_{di})}{\omega_A^2} \right]^{-1/2} \quad (\text{II.24})$$

with the low frequency ($|\omega| < \hat{\omega}_{*e}$) root

$$\omega \approx i \frac{\epsilon_\eta \omega_A^3}{|\omega_{di} \hat{\omega}_{*e}|} \left[1 + \frac{4\lambda_H}{\Gamma(1/4)} \sqrt{\frac{\hat{\omega}_{*e}}{\epsilon_\eta \omega_A}} \exp\left(i\frac{\pi}{4}\right) \right] \quad (\text{II.25})$$

indicating that the mode tends toward stability as λ_H becomes more negative.

Recently, a slightly different form of this dispersion relation was written [35] by simple re-arrangement:

$$\hat{C}_0 \delta = \lambda_H \frac{Q}{Q-1} H(Q) \quad (\text{II.26})$$

where $\hat{C}_0 \equiv 2\Gamma(5/4)/\Gamma(3/4)$, and

$$H(Q) = \frac{\Gamma[(Q+3)/4]\Gamma(5/4)}{\Gamma[(Q+5)/4]\Gamma(3/4)} \quad (\text{II.27})$$

This form of the dispersion relation permits far more accurate analytic estimates of the eigenfrequency in regimes where $|Q| < 1$, since it avoids the singularity in the Γ -function. It also has the advantage of allowing a simple approximation of the dispersion relation, obtained by setting $H(Q)=1$, to describe a wide variety of regimes (note that $H(Q \rightarrow 0)=1$, while $H(Q \rightarrow \infty) \approx 0.75$). This approximate form reads:

$$i(\omega - \hat{\omega}_{*e})\delta = \frac{\hat{C}_0}{\lambda_H} [\epsilon_\eta \omega_A + i\delta^2(\omega - \hat{\omega}_{*e})] \quad (\text{II.28})$$

Taking $|\lambda_H| \ll 1$ yields:

$$\epsilon_\eta \omega_A + i\delta^2(\omega - \hat{\omega}_{*e}) = 0 \quad (\text{II.29})$$

which can be rewritten as $i\epsilon_\eta \omega_A^3 = \omega(\omega - \omega_{di})(\omega - \hat{\omega}_{*e})$, namely the well-known [5] dispersion relation at ideal-MHD marginal stability.

If one wants to consider modes with $|\omega| < \hat{\omega}_{*e}$, Eq. (II.28) immediately approximates to a quadratic equation in $\delta \approx (-i\epsilon_\eta \omega \omega_{di} / \omega_A \hat{\omega}_{*e})^{1/4}$, whose solution yields:

$$(-i\omega)^{1/4} = (\gamma_{R*})^{1/4} \left\{ \left[1 + \frac{i\hat{\omega}_{*e}}{4\epsilon_\eta \omega_A} \left(\frac{\lambda_H}{\hat{C}_0} \right)^2 \right]^{1/2} + \left(\frac{i\hat{\omega}_{*e}}{4\epsilon_\eta \omega_A} \right)^{1/2} \frac{\lambda_H}{\hat{C}_0} \right\} \quad (\text{II.30})$$

where $\gamma_{R*} \equiv \epsilon_\eta \omega_A^3 / |\omega_{di} \hat{\omega}_{*e}|$ is the growth rate of the resistive internal kink in the presence of finite ion diamagnetic and electron drift frequency. From Eq. (II.30), we predict that

this resistive mode will stabilize for $\lambda_H < -2\hat{C}_0\sqrt{\epsilon_\eta\omega_A/\hat{\omega}_{*e}}$, a condition that is remarkably well verified by the numerical solution of Eq. (II.26). This stabilization of the resistive internal kink, which was suggested by Eq. (II.25), occurs at negative values of λ_H (\leftrightarrow low β_p), where the magnetic field line bending makes the perturbation energetically “costly” to the system. In order for this mode to become stable, a finite electron drift wave frequency ($\hat{\omega}_{*e}$) is required [35]. Although a non-vanishing ion diamagnetic frequency (ω_{di}) helps, it is not essential for stabilization, as was show numerically in Ref. [35].

Conversely, taking $\epsilon_\eta\omega_A > |\delta^2(\omega - \hat{\omega}_{*e})|$ in Eq. (II.28) and, looking for solutions with $\omega \approx \hat{\omega}_{*e}$ (so-called drift-tearing mode [36]), we obtain the growth rate:

$$\gamma \approx \gamma_{DT} \left\{ 1 - 2 \left(\frac{\hat{C}_0}{|\lambda_H|} \right)^{2/3} \left[\frac{\hat{\omega}_{*e}(\hat{\omega}_{*e} - \omega_{di})}{\omega_A^2} \right]^{1/3} \right\} \quad (\text{II.31})$$

where $\gamma_{DT} \equiv (\epsilon_\eta\omega_A/2)[\hat{\omega}_{*e}(\hat{\omega}_{*e} - \omega_{di})/\omega_A^2]^{-2/3}(\hat{C}_0/\lambda_H)^{4/3}$ is the drift-tearing growth rate. Here also, a marginal stability condition is indicated for λ_H smaller in absolute value than a critical value (cf. Eq. (II.31)) which is quite close to that found numerically from Eq. (II.26). The stabilization of the drift-tearing mode has been linked [35] to the progressive shielding of the perturbation within the singular layer from the ideal-MHD region, which “drives” the instability (breakdown of the “constant- ψ ” approximation).

A stability diagram in $\Omega_* - \hat{\lambda}_H$ space, where $\Omega_* \equiv \hat{\omega}_{*e}/\epsilon_\eta^{1/3}\omega_A$ and $\hat{\lambda}_H \equiv \lambda_H/\epsilon_\eta^{1/3}$, is shown in Fig. 1; the solid curves indicate points of marginal stability, $\gamma = \text{Im}(\omega) = 0$. The stable region, $\gamma < 0$ is located above each curve, for a given value of $1/\tau = -\omega_{di}/\hat{\omega}_{*e}$. Note, as discussed above, that finite- ω_{di} is not essential; a stable region is encountered (albeit reduced in size) even for $\tau = 0$. As can be seen from Eq. (II.31), the drift tearing mode has a marginal stability point even for $\omega_{di} = 0$ (it occurs for smaller $|\lambda_H|$, hence

“later” as far as the mode is concerned since we are moving inward from $\lambda_H = -\infty$). The resistive internal kink, on the other hand, obeys:

$$(-i\omega)^{1/2} = \left(\frac{\omega_A^3}{\epsilon_\eta \hat{\omega}_{*e}} \right)^{1/2} \exp(-i\frac{\pi}{4}) \left\{ \left[1 + \frac{i\hat{\omega}_{*e}}{4\epsilon_\eta \omega_A} \left(\frac{\lambda_H}{\hat{C}_0} \right)^2 \right] + \frac{\lambda_H}{2\hat{C}_0} \left(\frac{\hat{\omega}_{*e}}{\epsilon_\eta \omega_A} \right)^{1/2} \exp(i\frac{\pi}{4}) \right\} \quad (\text{II.30}')$$

for $\omega_{di} = 0$, indicating that stabilization is possible for this mode as well. Note that the characteristic growth rate scales as $\gamma'_{R*} \sim \epsilon_\eta^{-1}$ in this case.

II.3 Influence of ion-ion collisions.

When collisional ion-ion viscosity is taken into account ($\nu_\mu \neq 0$ in Eq. (II.16)), the numerical solution of the dispersion equation is no more difficult than before. Unfortunately, there exist no general analytic solutions to this equation. Viscosity represents an energy sink for the modes considered in this section: its influence is always stabilizing. By itself, the effect is not significant: viscosity tends to lower the growth rates of the tearing mode ($\gamma \approx \epsilon_\eta^{3/5} |\lambda_H|^{-4/5} \omega_A$) and of the resistive internal kink ($\gamma \approx \epsilon_\eta^{1/3} \omega_A$) when $\hat{\omega}_{*e} = \omega_{di} = 0$, but never leads to complete stability. This was shown explicitly, e.g. in [5] and [37], where a list of the various asymptotic regimes was presented along with the scaling of the relevant growth rates and widths of the singular layers.

In combination with finite ion diamagnetic frequency, viscosity can be an effective stabilizing agent for the resistive internal kink. A model dispersion relation can be written as:

$$(\omega + i\nu_\mu/2\lambda_H^2)(\omega - \omega_{di}) = -\lambda_H^2 \omega_A^2 - (5i/2)\epsilon_\eta \omega_A^3 / (\omega - \hat{\omega}_{*e}) \quad (\text{II.32})$$

This equation, which correctly reproduces the results for the more complete solution of Eq. (II.16) in the limit $\nu_\mu \sim \epsilon_\eta \omega_A < \lambda_H \omega_A < \omega_{di}$, bears a striking resemblance (apart

from the ϵ_η term) to the dispersion relation for electrostatic modes in the presence of ion-ion collisions, derived by Coppi and Rosenbluth (cf., unnumbered equation, obtained from Eq. (34) of [38] for the case of vanishing magnetic shear). That paper showed examples in which these electrostatic modes could be stabilized by ion-ion collisions for sufficiently high temperatures. The stabilization criterion for electromagnetic $m^0 = 1$ modes was first derived [39] by direct solution of Eq. (II.16). There it was shown that stability can occur for $D \equiv \nu_\mu / \epsilon_\eta \omega_A > D_{cr}$ where $D_{cr} < 1$ when $|\omega_{di}| > \omega_A \epsilon_\eta^{1/3}$, and the regularization of the eigenfunction by the presence of ν_μ was explicitly demonstrated. A fit of the numerical results, for $\hat{\omega}_{*e} = -\omega_{di}$, in the limit of large $|\omega_{di}| / (\omega_A \epsilon_\eta^{1/3})$ gives:

$$D_{cr} \equiv \frac{\nu_\mu}{\epsilon_\eta \omega_A} \Big|_e^{cr} = 8 \epsilon_\eta \left(\frac{\omega_A}{\hat{\omega}_{*e}} \right)^3 \left[1 + \frac{5}{8} \frac{\lambda_H^2 \hat{\omega}_{*e}}{\epsilon_\eta \omega_A} \text{sgn}(\lambda_H) \right] \quad (\text{II.33})$$

Since $D \propto \nu_{ii} \rho_i / \nu_{ie} \propto T$, one is tempted to conclude that increasing the plasma temperature would automatically lead to stabilization, when combined with finite diamagnetic frequency. Unfortunately, this does not appear to be the case for two reasons. First, as T_i is increased, the ion Larmor radius becomes comparable to the width of the singular layer, thereby invalidating the fluid treatment. As we shall see in the next section, finite Larmor radius (FLR) can provide a means to decouple the ion and electron motion in the direction perpendicular to the magnetic field. Maintaining the condition of quasi-neutrality then necessarily requires a parallel compression of the electron fluid, i.e. a non-zero parallel electric field. This provides a new instability regime for the internal kink, with a growth rate determined by the parameter ρ_i / r_s .

Second, as T_e is increased, classical electrical resistivity effectively drops out of Ohm's law and, in its place, one must now consider finite electron inertia.

II.4 Weakly collisional and collisionless limits

The generalized version of Ohm's law in the parallel direction reads:

$$E_{\parallel} = \eta_{\parallel} J_{\parallel} + \frac{4\pi}{\omega_{pe}^2} \frac{dJ_{\parallel}}{dt} - \frac{\nabla_{\parallel} p_e}{en} \quad (\text{II.34})$$

where the thermo-electric effect has been omitted, for simplicity. The new term appears in second position within the right side of this equation, and one generally writes: $d/dt = \partial/\partial t + \mathbf{V} \cdot \nabla$, where \mathbf{V} is the macroscopic fluid velocity.

The effect of $\partial J_{\parallel}/\partial t$ has been considered in two recent papers [40]-[41]. In the first, [40], the linear stability of $m^0 = 1$ modes with Eq. (II.33) replacing the classical Ohm's law has been examined with and without diamagnetic frequency effects. In the small ion Larmor radius limit (and $\omega_{di} = 0$), the following dispersion relation is obtained at ideal-MHD marginal stability ($\lambda_H = 0$):

$$\frac{\gamma}{\omega_A} = \frac{c}{\omega_{pe} r_s} \left(1 + \frac{\nu_{ei}}{\gamma}\right)^{1/2} \quad (\text{II.35})$$

In the limit of vanishing electrical resistivity, $\nu_{ei} \rightarrow 0$, this reproduces the result of an earlier paper [42] where an instability with growth rate proportional to the normalized electron collisionless skin depth was predicted. The presence of the ion gyro-radius ($\rho_s \equiv \sqrt{T_e/m_i}/\Omega_i$, which appears through the ion polarization drift) provides a new regime [43] for the growth rate in the collisionless limit (and $\omega_{di} = \hat{\omega}_{*e} = 0$), for small values of $|\lambda_H|$:

$$\gamma \approx \omega_A \frac{1}{r_s} (d\rho_i^2)^{1/3} \quad (\text{II.36})$$

where $d \equiv c/\omega_{pe}$ is the collisionless electron skin depth. This regime was first found by Drake [43] and denoted "modified collisionless tearing". The use of Padé's expression,

to approximate [44] the full FLR ion response by a two terms expression that correctly reproduces the full response in the small and large ion gyro-radius limits, only changes the above result by [40] $\rho_i^2 \rightarrow \rho_i^2(1 + T_e/T_i)$. When $\hat{\omega}_{*e}$ and/or ω_{di} are finite there exist regimes where diamagnetic stabilization of the ideal mode is still possible.

In the second of these two papers, [41], the same form of Ohm's law has been incorporated in a numerical simulation of the coalescence of two magnetic flux bundles, also for $\hat{\omega}_{*e} = \omega_{di} = 0$. The resulting collapse of the current channel into a layer smaller than the collisionless skin depth has led the authors to theorize the appearance of a microinstability (the "current convective" instability) which then provides an anomalous diffusion in the direction perpendicular to the magnetic field (this work follows an analysis [45] in which conditions for the instability of a narrow current sheet, embedded in a sheared magnetic field, against extremely high poloidal wavenumber micro-tearing modes were derived). Scalings for the inflow velocity and the width of the current layer have been obtained [41] in terms of V_A , d , $\beta m_i/m_e$, and a (the minor radius), and a fast collapse time ($\tau \sim 40 \mu\text{sec}$ for TFTR, commensurate with the prediction of Ref. [40], cf. Eq. (II.36)) has been predicted.

Finally, Wesson [46] has considered the other component of the electron inertia term, namely using $\mathbf{V} \cdot \nabla J_{\parallel}$ instead of the explicit time derivative of J_{\parallel} in Eq. (II.34). This term is expected to be dominant in nonlinear regimes. Using a line of reasoning analogous to that of Kadomtsev [3], Wesson shows how fast sawtooth crashes arise from this non-classical resistivity, in situations where both the ion diamagnetic and electron drift wave frequencies are negligible.

III. Kinetic Theory within the Singular Layer

As discussed in the previous section, cf. Table I, present-day experiments operate in parameter regimes in which at least one of the relevant inequalities (required for validity of the two-fluid theory) is violated. Indeed, we have seen that the conditions for fluid treatment of electrons and ions, when reduced to conditions on the thickness of the singular layer, can be mutually exclusive, thereby requiring that at least one species be treated kinetically. The formal derivation of the kinetic equations for $m^0 = 1$ modes is a task rendered formidable by the fact that, unlike the case of high $m^0 = n^0 q$ modes, an eikonal representation of perturbed quantities is in general not justified and the perpendicular “wavevector” is an operator. However, if one is interested in describing the physics within the singular region (where the eigenfunction varies over scale lengths much shorter than r_s , itself smaller than the scale length for variation of equilibrium quantities), one can use standard kinetic equations as found, e.g., in [47].

III.1 Kinetic electrons

Probably the first analysis of kinetic effects on the stability of internal kinks can be found in [43] and [48]. The ion dynamics were computed via a fluid theory, keeping only the $\mathbf{E} \times \mathbf{B}$ and polarization drifts (neglecting FLR corrections). Kinetic effects were retained in the electron dynamics where a Fokker-Planck equation, with a pitch-angle scattering operator, was solved. The concept of a Doppler frequency was introduced, a frequency which reduces to $\omega_D \approx k_{\parallel}(x)V_{Te}$ in the case of free-streaming (collisionless) electrons, and to $\omega_D \approx k_{\parallel}^2(x)V_{Te}^2/\nu_e$ in the case of parallel diffusing (collisional) electrons. In all cases, ω_D appears in a velocity integral and is velocity dependent ($V_{Te} \rightarrow v$, $\nu_e \rightarrow$

$\nu_e(V_{Te}/v)^3$ in the above expressions). Thus, the presence of the Doppler frequency brings about modifications to the temperature gradient contributions due to the effective drift wave frequency, $\omega_{*e}^T(v) = \omega_{*e}[1 - \eta_e(3/2 - v^2/V_{Te}^2)]$, where $\omega_{*e} = (cT_e/eBnr_s)(dn/dr)$ is the electron diamagnetic frequency, and $\eta_e = d \ln T_e/d \ln n$ is the contribution from the temperature gradient. These modifications, in turn, cause the appearance of instabilities of drift-tearing modes caused exclusively by ∇T_e . It was found [43] that, apart from the appearance of these ∇T_e instabilities, electron Doppler (kinetic) effects have no substantial effects for $\lambda_H > (\rho_i/r_s)\sqrt{T_e/T_i}$. The ∇T_e mode exists as an instability in collisional regimes, $\nu_e > |\omega|$, propagates with $Re(\omega) \approx \omega_{*e}(1 + 5\eta_e/2)$ and requires (cf. Eq. (34b) of Ref. [43]):

$$\epsilon_\eta \leq 3 \frac{d}{r_s} \left(\frac{\omega_{*e}}{\omega_A} \right)^2 \quad (\text{III.1})$$

where d is the collisionless skin depth mentioned previously. Estimating $\nu_{ei} > |\omega| \sim 3\omega_{*e}$, this inequality requires $(2r_s/d)(\omega_{*e}/\omega_A) > 1$, which makes this mode relevant to rather large machines ($r_s > 30$ cm).

In the collisionless limit, the streaming of the electrons (finite $\omega/k_{\parallel}V_{Te}$) provides an effective longitudinal conductivity and an instability of the $m^0 = 1$ mode is found with $\gamma \approx \omega_A d/r_s$ when both λ_H and ω_{*e} are negligible, cf. [42], [43], [48]. When λ_H is negative and finite, weak instabilities of the “reconnecting” mode [5] appear with $Re(\omega) \sim \omega_{*e}$. In this regime, the so-called “constant- ψ ” approximation has been applied. This model has been generalized to cover arbitrary values of ρ_i/r_s in [49]-[50], where a trend toward stabilization of this reconnecting mode was observed. The opposite effect (of finite ρ_i/r_s) was found for the collisionless internal kink (which does not obey the “constant- ψ ” approximation), in

regimes where $\lambda_H \geq 0$: FLR enhances instability of this mode [51]. This later study made use of quadratic forms which employed trial functions adapted from known [42] solutions obtained for $\lambda_H = 0$. This enhancement of the growth rate was related to the property that, when $|\lambda_H| < \rho_i/r_s$, the ion Larmor radius defines the minimal size of the singular layer where tearing and reconnection occur.

Electron kinetic effects are encountered in a sub-layer where $k_{\parallel}^2 V_{Te}^2 \sim \nu_{ei} |\omega|$ for collisional regimes ($\nu_{ei} > |\omega|$), or where $k_{\parallel}(x) V_{Te} \leq |\omega|$, for collisionless regimes. In either case, $|k_{\parallel}|$ is an increasing function of x , the distance from the $q = 1$ surface. This makes a treatment in x -space the most convenient method for solution of the electron dynamics (i.e., determination of the electron parallel conductivity, $\sigma(x, \omega)$). Unfortunately, the ion dynamics are most easily treated in conjugate (i.e., k -) space, especially in full FLR regimes. We shall return to a discussion of this rather formidable problem later in this section.

III.2 Kinetic ions

In order to more carefully study the effects of ion FLR, a mixed analysis was performed [44] where perpendicular ion dynamics were determined via kinetic theory (parallel dynamics are neglected in regimes where $|\omega| > k_{\parallel} V_{Ti}$):

$$\frac{\hat{n}_k}{n} = \left[\frac{\hat{\omega}_{*e}}{\omega} - D_b(b \equiv k^2 \rho_i^2 / r_s^2) \right] \frac{e \hat{\phi}_k}{T_e} \quad (\text{III.2})$$

where the subscript k indicates the Fourier transform of a given quantity and the non-local portion of the ion response is contained within

$$D_b(b) = \frac{\hat{\omega}_{*e}}{\omega} + \tau [1 - \Gamma_0(b)] - \frac{\hat{\omega}_{*e}}{\omega} \Gamma_0(b) (1 - \eta_i M) \quad (\text{III.3})$$

where $\tau \equiv T_e/T_i$, $M \equiv b[1 - I_1(b)/I_0(b)]$, $\Gamma_0(b) = I_0(b) \exp(b)$, $I_{0,1}$ are modified Bessel functions, and $\eta_i = d \ln T_i / d \ln n$. The electron dynamics ($\mathbf{E} \times \mathbf{B}$ drift perpendicular to the magnetic field and compressible parallel motion) are assumed to be governed by fluid equations in the isothermal limit ($k_{\parallel}^2 V_{Te}^2 \gg |\omega| \nu_e \rightarrow$ no electron temperature perturbation):

$$\frac{\hat{n}_k}{n} = \frac{\hat{\omega}_{*e}}{\omega} \frac{e\hat{\phi}_k}{T_e} + i \frac{\omega_A}{\omega} \frac{d}{dk} \hat{J} \quad (\text{III.4})$$

where $\hat{J} \equiv -\hat{v}_{\parallel e}(k)/V_A$ represents the perturbation of the parallel current (related to the electromagnetic potential through Ampere's law). Ohm's law takes the form:

$$\left(\frac{\epsilon_{\eta} \tau_s^2}{\tau \rho_i^2} - i \frac{\omega_A}{\omega} \frac{d^2}{dk^2} \right) \hat{J} = \left(1 - \frac{\hat{\omega}_{*e}}{\omega} \right) \hat{E}_k \quad (\text{III.5})$$

and \hat{E}_k is the Fourier transform of the perturbed parallel electric field ($E_{\parallel} = -\nabla_{\parallel} \phi - (1/c)dA_{\parallel}/dt$). The resulting dispersion relation,

$$\frac{d}{dk} \left(1 + \frac{1 - \hat{\omega}_{*e}/\omega}{D_b} \right) \frac{d\hat{J}}{dk} - \left(1 - \frac{\hat{\omega}_{*e}}{\omega} \right) k_{\rho}^2 \left(\frac{1}{k_J^4} + \frac{1}{k^2 k_A^2} \right) \hat{J} = 0 \quad (\text{III.6})$$

is written in terms of the three characteristic "lengths" in Fourier space. The inertial length

$$k_A^2 = - \frac{\omega_A^2}{\omega(\omega - \hat{\omega}_{*e})} \quad (\text{III.7 - a})$$

the FLR length

$$k_{\rho}^2 = \frac{1}{\tau \rho_i^2} \frac{\omega}{\omega - \omega_{di}} \quad (\text{III.7 - b})$$

and the resistive length

$$k_J^4 = \frac{i\omega_A}{\epsilon_{\eta} \omega} \frac{\omega - \hat{\omega}_{*e}}{\omega - \omega_{di}} \quad (\text{III.7 - c})$$

The parallel perturbed current satisfies the boundary condition:

$$\hat{j} \rightarrow 1 - \frac{k^2}{2k_A^2} + \frac{1}{3}\lambda_H \frac{k^3}{k_A^2} \text{sgn}(k) \quad (\text{III.8})$$

for k smaller than the largest of the three lengths indicated in Eq. (III.7).

The use of the isothermal approximation, $|k_{\parallel}^2 V_{Te}^2 / \nu_{ei} \omega| \gg 1$, was made [44] instead of the more commonly used adiabatic equation of state (cf. Eq. (II.12) and [4]-[5]) in order to describe weakly collisional regimes. Since k_{\parallel} varies linearly with the distance from the $q = 1$ surface, there will be an inner sub-layer where the isothermal approximation breaks down. For the resistive internal kink, the half-width of this sub-layer may be estimated to be $x \leq x_e \sim \epsilon_{\eta}^{1/6} (V_A \nu_{ei} R)^{1/2} / [V_{Te} s(r_s)]$ in the absence of diamagnetic frequency, and $x_e \sim \epsilon_{\eta}^{1/2} (V_A / V_{Te}) (V_A \nu_{ei} / R)^{1/2} / [\hat{\omega}_{*e} s(r_s)]$ when effects due to $|\omega_{di}| \sim \hat{\omega}_{*e}$ are important. Note that $x_e \propto 1/s(r_s) = 1/r_s q'(r_s)$, so that low magnetic shear tends to reduce the width of this sub-layer. Formally then, one should solve the equations within the singular layer in two domains, one where the isothermal approximation holds, and the other (the “sub-layer”) where electron kinetic effects are important, and subsequently match the two solutions. Such an approach was taken for the drift-tearing mode [52] with $\omega \approx \hat{\omega}_{*e}$, for which the use of the constant- ψ approximation is justified. No such approximation can be made for the lower frequency internal kink, and the authors of Ref. [44] made the tacit assumption that the sub-layer was small enough that it effectively could be ignored. Now, if $x_e < \max(1/k_A, 1/k_{\rho}, 1/k_J)$, this may well be a good description. This is the situation, e.g., for supershots in TFTR and ICRH (ion cyclotron resonance heating) in JET (cf. Table I and Refs. [24], [26]), where $x_e \approx 2 \cdot 10^{-4}$, while $1/k_{\rho} \sim 0.3$ (given that $|\omega| \ll \hat{\omega}_{*e}$).

With this limitation in mind, one can solve the dispersion equation (III.6), in the semi-collisional regime $k_J^2 > |(1 - \hat{\omega}_{*e}/\omega)(1 - \omega_{di}/\omega)|(1 + 1/\tau)k_\rho^2$ and for low values of η_i . Using an approximate form for D_b , valid for both small and large values of $b = k^2 \rho_i^2$ (i.e., a Padé approximant), one obtains an analytic dispersion relation (Eq. (11) of Ref. [44]). In the limit of vanishing resistivity and large gyroradius ($k_\rho^2 < k_A^2$), the dispersion relation reduces to:

$$\omega(\omega - \hat{\omega}_{*e})(\omega - \omega_{di})^2 = \left(\frac{2\lambda_H}{\pi}\right)^2 (1 + \tau) \left(\frac{\rho_i}{r_s}\right)^2 \omega_A^4 \quad (\text{III.9})$$

so that an unstable mode with $\gamma = (2\lambda_H \rho_i / \pi r_s)^{1/2} (1 + \tau)^{1/4} \omega_A$ appears for $|\omega_{di}| = \hat{\omega}_{*e} \rightarrow 0$. For $\lambda_H \rho_i \omega_A \ll \hat{\omega}_{*e} r_s$ the instability disappears through the same process of FLR stabilization found originally in the fluid theory [4]-[5]. Since $k_\rho^2 < k_A^2$ implies $\rho_i > \lambda_H r_s$ in the absence of diamagnetic effects, the growth rate is enhanced over the corresponding value found in the small gyroradius limit ($\gamma = \lambda_H \omega_A$). Similarly, the resistive internal kink appears with a different growth rate in the large Larmor radius regime [44]: $\gamma = [2(1 + \tau)]^{2/7} \epsilon_\eta^{1/7} (r_s / \rho_i)^{3/7}$. Solutions of Eq. (III.6), using the full form of D_b , confirm [44] the overall destabilizing influence of finite ion gyroradius, establish an overall stabilizing influence of the ion temperature gradient ($\eta_i > 0$) on the resistive internal kink, and indicate that, for η_i above a threshold value (approximately 1.65), a weakly unstable “ion temperature gradient mode” appears (albeit with an extremely low oscillation frequency, $Re(\omega) \ll |\omega_{di}|$).

The role of the ion temperature gradient parameter, η_i , must be considered with caution. The authors of Ref. [44] show diagrams (normalized growth rate vs. normalized ω_{di} , cf. Figs. 2-4 in that paper) which indicate that a smaller ion diamagnetic frequency

$\omega_{*i} \propto dn/dr$ is needed to stabilize the resistive internal kink if η_i is increased: clearly a stabilizing effect. On the other hand, the authors of Ref. [51] choose to normalize their parameters in such a way as to maintain the zero-FLR limit of their equations invariant to changes in, e.g., η_i and $\tau = T_e/T_i$. Thus they conclude that a larger total pressure gradient, cf. their parameter $\hat{\beta} = [\omega_{*i}(1 + \eta_i)/2\omega_A]^2$, is needed to stabilize the mode for larger temperature gradients (the relative positions of the curves marked $\eta_i = 0, 2, 4$ in Fig. 4 of Ref. [51] would become reversed if plotted against $\hat{\beta} = \omega_{*i}/\omega_A$). Since the equilibrium temperature gradient also affects parameters such as λ_H (through the poloidal beta, cf. [10], [20]) which increases with $|dp_i/dr|$, the role of η_i is by no means obvious. If β_p is much smaller than the critical value at which $\lambda_H = 0$, then λ_H is essentially unaffected by η_i and one is allowed to conclude, as in Ref. [44], that a smaller ion density gradient is needed to FLR stabilize the resistive internal kink (the rest of the stabilization being provided by the temperature gradient).

A numerical example of the behavior of the resistive internal kink is shown in Figs. 2-3. These figures are obtained by numerically solving Eq. (28) of Ref. [44], which is the dispersion relation obtained using full ion dynamics (i.e., without Padé's approximation) in a regime where the ion Larmor radius is much larger than the inertial width, and where resistivity is weak (cf. Eq. (31)-(32) of Ref. [44]). From these figures, one can see the same quantitative behavior as for the fluid theory (cf. the discussion near Eq. (II.30)-(II.31) in Sec. II): when $\Omega_* \equiv \hat{\omega}_{*e}/\epsilon_\eta^{1/3}\omega_A$ is large enough (≥ 3 for the parameters chosen here), the resistive internal kink stabilizes at large enough negative values of $\hat{\lambda}_H \equiv \lambda_H/\epsilon_\eta^{1/3}$. One then enters the stable regime that separates the resistive internal kink from the drift-

tearing mode. Below that critical value for Ω_* , the resistive kink connects in a continuous fashion with the drift-tearing root whose instability occurs with $Re(\omega) \approx \hat{\omega}_{*e}$, as shown in Figs. 2-3.

The model of Ref. [44] was extended to include collisionless regimes by using a generalized version of Ohm's law (though treating the electron response via fluid theory) : $\mathbf{E} = \eta\mathbf{J} + (4\pi/\omega_{pe}^2)\partial\mathbf{J}/\partial t - \nabla p_e/en$ in Ref. [40]. This topic has been discussed in Sec. II in some detail; we simply remember here that a new, hybrid, growth rate was found in the collisionless large Larmor radius regime, $\gamma \approx \omega_A (c\rho_i^2/\omega_{pe}r_s^3)^{1/3}$, provided $\omega_{di} = \hat{\omega}_{*e} = 0$. This collisionless instability is subject to stabilization by finite ion diamagnetic and electron drift wave frequency, just like the instability of the ideal kink in the fluid regime.

The kinetic model for the ions was extended [53] to include the stabilizing effect of ion-ion collisional viscosity. A particle and momentum conserving collisional operator [38] was introduced for this purpose. The hitherto unexplored regime, $\rho_i \leq \epsilon_\eta^{1/3} r_s$, was studied numerically and a non-monotonic dependence of the growth rate on the ion Larmor radius was found: as ρ_i/r_s increases, from zero, the mode frequency experiences a downshift from its starting value. This downshift renders diamagnetic stabilization (by finite $|\omega_{di}|$) more effective, and the growth rate decreases at first. As ρ_i is further increased, the growth rate reaches a minimum value and then reverses direction (increases) as the destabilization takes over due to the fact that the ion Larmor radius defines the singular layer width when $\rho_i > \epsilon_\eta^{1/3} r_s$.

III.3 Kinetic electrons and ions

The simultaneous use of an isothermal equation of state for the electrons (valid, in

principle, only for $k_{\parallel}^2 V_{Te}^2 \gg |\omega \nu_e|$), and the resistive form of Ohm's law, e.g., Eq. (II.15) or Eq. (6) in Ref. [44], is problematic in that regimes where $\epsilon_{\eta}/\tau \rho_i^2 \sim |\omega_A/\omega|$ cannot be explored. A generalized electron conductivity, $\sigma(x, \omega)$, has been used in [54] to explore arbitrary values of electron collisionality, in the absence of equilibrium temperature gradients ($\eta_i = \eta_e = 0$). By first considering a Lorentzian conductivity model

$$\sigma(x) = \tau \left(\frac{r_s}{\rho_i} \right)^2 \frac{\omega(\omega - \omega_{*e})}{\omega_A^2} \frac{x^2}{2x_r^2 - x^2} \quad (\text{III.10})$$

with

$$x_r^2 \equiv \frac{\omega(\omega + i\nu_e)}{(k'_{\parallel} L_n)^2} \quad (\text{III.11})$$

and $k'_{\parallel} = s(r_s)/R$ (L_n is the density gradient scale length), as well as a Padé approximant (cf. [44]) for the ion response, an analytic solution to the stability problem was obtained [54] for regimes which verify

$$\tau \frac{m_e}{m_i} \ll \beta_i \ll \frac{1}{(2k'_{\parallel} L_n)^2} \quad (\text{III.12})$$

The right side of this inequality can also be written as $\omega_{di}/\omega_A < \rho_i/\tau_s$ and is equivalent to the limit $|(1 - \hat{\omega}_{*e}/\omega)z_{\rho}^2/\mu z_A^2| \ll 1$ of Ref. [44] (using their notation). The left side of (III.12) makes the electron layer, where the conductivity is spatially varying, thin compared to the inertial width. The resulting dispersion relation is particularly simple (cf. Eqs. (50) and (A-14) of Ref. [54]):

$$-\lambda_H = i \frac{x_e^*}{\bar{\sigma}} + \frac{\pi \sqrt{\bar{\sigma}}}{2k_A} \quad (\text{III.13})$$

where $\bar{\sigma} = [2(\omega - \omega_{*i})(\omega - \omega_{*e})/(1 + \tau)](\beta_i/4)(1/k'_{\parallel} L_n)^2 \ll 1$, and $x_e^* = (2m_e/m_i \beta_i)^{1/2} [(\omega + i\nu_e)/\omega_A(1 + \tau)]^{1/2}/k_A$ is the effective electron layer width.

Provided that the inequalities in (III.12) are verified, the dispersion relation given by Eq. (III.13) can also be obtained [54] with other forms of the electrical conductivity (i.e., not Lorentzian). This then justifies the use of the isothermal equation of state (cf. [44]) in the prescribed parameter regime. The dispersion relation, Eq. (51) of Ref. [54], agrees with that of Ref. [44] (i.e., Eq. (28) in the limit $\eta_i = 0$, see their Appendix C), provided the dissipative term is modified appropriately:

$$\epsilon_\eta \rightarrow \left(\frac{2}{\pi}\right) \left(\frac{\rho_i}{r_s}\right)^2 \frac{\omega}{\omega_A} \frac{\omega(\omega + i\nu_e)}{(k'_\parallel V_{Te})^2} \quad (\text{III.14})$$

in going from Ref. [44] to Ref. [54].

We conclude this section by presenting a table of estimates for the growth times, for various experiments, as they arise from resistive theory [4]-[5], drift-modified resistive theory [4]-[5], collisionless theory [42], and collisionless-FLR theory [40]. The symbol “n/a” appears in two locations to indicate that the particular time scale is of no relevance, since $|\omega_{di}|$ and/or $\hat{\omega}_{*e}$ are smaller than $\epsilon_\eta^{1/3} \omega_A$ (violating basic orderings of the theory). The symbol “ ∞ ” is used to indicate that the model predicts linear stability ($\gamma < 0$). As can be seen, none of the models of Table II is able to yield the fast ($\tau \leq 100 \mu\text{sec}$) time scales necessary to explain sawtooth crashes in large experiments. Note that the “FLR collisionless time” shown in the third column is computed with $\omega_{di} = \hat{\omega}_{*e} = 0$, and, thus is not an experimentally relevant time scale (it is presented here as an illustrative example). If one assumes complete flattening of the pressure gradient at the $q = 1$ surface (by, e.g., the presence of a magnetic island due to a finite size perturbation), then both the “collisionless time” and the time scale indicated in Ref. [40], $\tau = (\omega_{pe}/c\rho_i^2)^{1/3}/\omega_A$ ($\sim 40 \mu\text{sec}$ for TFTR; see also [41]) would be relevant and help explain these fast crashes.

IV. Energetic Particles

The concept of using a population of energetic particles as an “anchor” for the purpose of stabilization has a long history. Among the earliest experiments, for which such a scheme was proposed, were the Astron [55], ion rings [56], and the ELMO Bumpy Torus [57]. A concise and elegant paper [58] showed how high- $n^0 q$ ballooning modes could be stabilized by energetic trapped particles whose response to perturbation would differ from the rest of the fluid.

In retrospect, it is not surprising that similar arguments could be applied to $m^0 = n^0 = 1$ modes, the more so because these perturbations act principally as rigid displacements of the entire inner portion ($q(r) \leq 1$) of the plasma column. If a particular species does not follow the column in its helical deformation (cf., Fig. 6.3 of Ref. [59]), and that species has a density gradient in the radial direction, a charge separation is set up with an electric field that produces an $\mathbf{E} \times \mathbf{B}$ torque on the fluid, and that opposes the original motion. The initial indication that such considerations were more than of an academic nature came from high-power ion cyclotron heating (ICRH) experiments in JET [60]-[62], as well as later in TEXTOR [63] and in TFTR [64]. In these experiments, sawtooth-free periods of up to several seconds were observed, and their appearance has been conclusively [62], [65] been associated with the presence of energetic ions. These ions arise from either ICRH or neutral beam (NB) heating. It is important to distinguish these sawtooth suppression experiments from others, such as those performed in ASDEX [66], T-10 [67], or JT-60 [68], where stabilization was achieved by modification of the current density profile via electron cyclotron heating (ECH), or by operating in a lower hybrid current drive mode

$(q_0 \equiv q(r = 0) \geq 1)$.

Historically, the association between energetic particles and $m^0 = 1$ modes arose in a different manner, namely through the discovery of the phenomenon called “fishbone oscillations”, first observed in PDX [69]-[71], then D-IIID [72]-[73], PBX [74], and TFTR [75]. These are high frequency (relative to the sawtooth repetition frequency) bursts of oscillations, observed either in the soft X-ray signals or in the Mirnov coils of the Tokamak, and which are associated with the turn-on of the neutral beams (or, in a milder form with that of ICRH in JET [76]). The two phenomena (sawteeth and fishbones) are related and there is a commonality in the effects of energetic particles. Yet, they represent different roots of a single dispersion relation and, thus, will be considered separately.

Let us begin with a simple illustration of the origin of the two roots. Consider the following model dispersion relation:

$$(\omega + i\nu)(\omega - \omega_{di}) = -\lambda_H^2 \omega_A^2 - \frac{5}{2}i \frac{\epsilon_\eta \omega_A^3}{\omega - \hat{\omega}_{*e}} \quad (\text{IV.1})$$

where ν is a constant dissipation rate which models either ion collisional viscosity (cf. Sec. II) or a wave-particle resonance. In the absence of resistivity, this equation has only two roots. When a finite amount of resistivity is introduced, a third root appears, with $\omega \approx \hat{\omega}_{*e}$. From a solution of the more complete dispersion equation (a differential equation in either x or k space), one can establish that this root is not spatially localized, hence we will not consider it of relevance here (it turns out that this mode can be localized by finite parallel electron conductivity [77], an effect which also tends to stabilize that mode). Let us consider a regime where $|\omega_{di}/\omega_A| > \lambda_H > \max(|\nu/\omega_{di}|, \epsilon_\eta)$. Then, a perturbative

analysis of the dispersion relation establishes the following two roots:

$$\omega = \lambda_H \frac{\omega_A^2}{\omega_{di}} - i\nu + \frac{5}{2} i \frac{\epsilon_\eta \omega_A^3}{|\omega_{di} \hat{\omega}_{*e}|} \quad (\text{IV.2 - a})$$

$$\omega = \omega_{di} \left(1 - \lambda_H^2 \frac{\omega_A^2}{\omega_{di}^2} \right) + i\nu \left(\lambda_H \frac{\omega_A}{\omega_{di}} \right)^2 - \frac{5}{2} i \frac{\epsilon_\eta \omega_A^3}{\omega_{di} (\omega_{di} - \hat{\omega}_{*e})} \quad (\text{IV.2 - b})$$

The first root is a low frequency mode (cf. our orderings) which is destabilized by resistivity (note that $\omega_{di} \hat{\omega}_{*e} < 0$), and is stabilized by the dissipation ($\nu > 0$ by convention, here). This is the root which is customarily associated with the sawtooth crash (the “precursor”). The second root occurs near the ion diamagnetic frequency, is destabilized by the dissipation (ν , though weakly) and feels a stabilizing influence by the resistivity. Note that considerations of growth or damping do not depend on the sign of ω_{di} , as should be expected. This picture is a clear example of dissipation working in opposite directions on modes which have opposite energy [78].

IV.1 The energetic particle functional ($\lambda_k \propto -\delta W_h$)

The derivation of the dispersion relation, including the effects of energetic particles, starts with the recognition that, typically, these particles have Larmor radii that are much larger than the characteristic thickness of the singular layer. As a consequence, their response within the layer is adiabatic ($k_r \rho_h \gg 1$) and they introduce no new physics there. In order to describe their response in the outer layer (which we termed the “ideal MHD region” up to now), we recall the linearized equation of motion:

$$-\omega^2 \rho \vec{\xi} = -\nabla \tilde{p}_c - \nabla \cdot \tilde{\mathbf{P}}_h + \frac{1}{\pi} [(\tilde{\mathbf{B}} \cdot \nabla) \mathbf{B} + (\mathbf{B} \cdot \nabla) \tilde{\mathbf{B}} - \nabla(\tilde{\mathbf{B}} \cdot \mathbf{B})] \quad (\text{IV.3})$$

as well as the equation for the magnetic perturbation

$$\tilde{\mathbf{B}} = \nabla \times (\vec{\xi} \times \mathbf{B}) \quad (\text{IV.4})$$

and a polytropic equation of state (with index Γ) for the core part of the plasma (i.e., the plasma minus the energetic species)

$$\tilde{P}_c = - \vec{\xi} \cdot \nabla p_c - \Gamma p_c \nabla \cdot \vec{\xi} \quad (\text{IV.5})$$

The energetic particle pressure tensor can be written in standard fashion:

$$\tilde{\vec{P}}_h = \tilde{p}_{\perp h} \hat{I} + (\tilde{p}_{\parallel} - \tilde{p}_{\perp})_h \hat{e}_{\parallel} \hat{e}_{\parallel} + (p_{\parallel} - p_{\perp})_h (\hat{e}_{\parallel} \tilde{\hat{e}}_h + \tilde{\hat{e}}_h \hat{e}_{\parallel}) \quad (\text{IV.6})$$

Since we are dealing with low frequency modes ($|\omega| \ll \Omega_i \equiv$ ion cyclotron frequency), the pressure tensor is diagonal and has only two components:

$$\tilde{p}_{\parallel h} = m_h \int d^3 v v_{\parallel}^2 \tilde{f}_h \quad (\text{IV.7 - a})$$

$$\tilde{p}_{\perp h} = m_h \int d^3 v \frac{v_{\perp}^2}{2} \tilde{f}_h \quad (\text{IV.7 - b})$$

where \tilde{f}_h is the gyrophase average of the perturbed distribution function. Note that, since we are in the “external region” and the energetic particles are few in number ($\tilde{p}_h \sim \epsilon_s^M \tilde{p}_c$ where $M = 1/2 \rightarrow 1$, $\nu = 1/2 \rightarrow 1$ and $\epsilon_s \equiv r_s/R$), the ideal MHD equations are used, to lowest order in ϵ_s , to relate field quantities (e.g., Eq. (IV.4) obtained from the ideal MHD version of Ohm’s law plus Faraday’s equation). We refer the reader to Ref. [79] for a detailed derivation of the dispersion relation; here we report only the salient portions. First, given the ordering on the pressures of the energetic and thermal particles, and given that the dispersion relation involves only terms of order $\epsilon_s^2 \tilde{p}_c$ (cf. Refs. [4]-[5] and Sec. II), terms involving energetic particles will need to be retained to order $\epsilon_s \tilde{p}_h$ only.

Let us begin by using $\tilde{\hat{e}}_{\parallel} = \tilde{\mathbf{B}}_{\perp}/B$ and writing

$$\begin{aligned} \nabla \cdot \tilde{\vec{P}}_h &= \nabla_{\perp} \tilde{p}_{\perp h} + \nabla_{\parallel} \tilde{p}_{\parallel h} + (\tilde{p}_{\parallel h} - \tilde{p}_{\perp h}) \vec{\kappa} \\ &\quad + \frac{1}{B} \hat{e}_{\parallel} (\tilde{\mathbf{B}}_{\perp} \cdot \nabla) (p_{\parallel} - p_{\perp})_h \end{aligned} \quad (\text{IV.8})$$

where $\vec{\kappa} \equiv (\hat{e}_{\parallel} \cdot \nabla) \hat{e}_{\parallel}$ is the magnetic curvature, and we have dropped terms of order $\nabla \cdot \hat{e}_{\parallel} \sim B_{\perp}/RB \sim \epsilon_s^2/r$ as well as $\hat{e}_{\parallel} \cdot \nabla \tilde{B}_{\perp}/B \sim \epsilon_s^2/R$. Operating with $\hat{e}_{\parallel} \cdot \nabla \times$ on the equation of motion (i.e., Eq. IV.3), this is the ‘‘annihilation operator’’ introduced in Ref. [29]), we obtain

$$0 = -4\pi \vec{\kappa} \cdot (\hat{e}_{\parallel} \times \nabla) (\tilde{p}_{\parallel} - \tilde{p}_{\perp})_h + \hat{e}_{\parallel} \cdot \nabla \times [(\mathbf{B} \cdot \nabla) \tilde{\mathbf{B}} + (\tilde{\mathbf{B}} \cdot \nabla) \mathbf{B}] \quad (\text{IV.9})$$

where the contribution from inertia has been disregarded ($\omega \sim \epsilon_s^2 \omega_A$, so that $(4\pi/B^2) \omega^2 \rho \hat{e}_{\parallel} \cdot \nabla \times \vec{\xi} \sim \epsilon_s^4 \xi_{\perp}/r$). The Lorentz term on the right hand side of Eq. (IV.9) can be evaluated explicitly to yield:

$$\begin{aligned} \hat{e}_{\parallel} \cdot \nabla \times [(\mathbf{B} \cdot \nabla) \tilde{\mathbf{B}} + (\tilde{\mathbf{B}} \cdot \nabla) \mathbf{B}] &= \frac{i}{m^0 r^2} \left[B^2 \frac{\partial}{\partial r} \left(r^3 F^2 \frac{\partial \xi_r}{\partial r} \right) \right. \\ &\quad \left. + 2im^0 r^2 B \hat{e}_{\parallel} \cdot (\vec{\kappa} \times \nabla) \tilde{B}_{\parallel} \right] \end{aligned} \quad (\text{IV.10})$$

In the derivation of this equation we have made use of the fact that $\tilde{B}_{\parallel} \sim \epsilon_s \tilde{B}_{\perp}$ (see below), so that $\nabla \cdot \tilde{\mathbf{B}}_{\perp} \sim \epsilon_s \tilde{B}_{\perp}$ and also have used $\tilde{B}_r = iF \xi_r$, where we remember that $F = \mathbf{k} \cdot \mathbf{B}$. Now, consider the radial component of Eq. (IV.3) to lowest order in ϵ_s ,

$$0 = \tilde{p}_c + \tilde{p}_{\perp h} + \frac{B \tilde{B}_{\parallel}}{4\pi} \quad (\text{IV.11})$$

which is equivalent to saying that the modes of interest are decoupled from the fast magnetosonic mode. Substituting Eq. (IV.10)-(IV.11) into (IV.9), we obtain:

$$\frac{\partial}{\partial r} \left(r^3 F^2 \frac{\partial \xi_r}{\partial r} \right) = 4\pi i m^0 r^2 (\hat{e}_{\parallel} \times \vec{\kappa}) \cdot \nabla (2\tilde{p}_c + \tilde{p}_{\perp h} + \tilde{p}_{\parallel h}) \quad (\text{IV.12})$$

Comparing this equation to Euler’s equation obtained from the ideal MHD energy principle, Eq. (II.2), and using Eq. (II.9), we find that the energetic particles contribute to the

exterior region through the functional:

$$\lambda_k(\omega) = - \frac{4\pi^2 i m^0}{\xi_\infty (B_\theta^2 s)_{r_s}} \int_0^{r_s} dr r^2 \int_0^{2\pi} \frac{d\theta}{2\pi} (\hat{e}_\parallel \times \bar{\kappa}) \cdot \nabla (\tilde{p}_\perp h + \tilde{p}_\parallel h) \times \exp [i (m^0 \theta - n^0 \zeta + \omega t)] \quad (\text{IV.13})$$

The contribution from $2\tilde{p}_c$ to Eq. (IV.12) is formally included in λ_H with all other (e.g., toroidal) contributions from the core species of the plasma. Thus, once $\lambda_k(\omega)$ is known, the dispersion relation for the resistive and/or ideal internal $m^0 = 1$ kink modes is obtained from Eq. (II.22) by direct substitution:

$$\left[- \frac{\omega (\omega - \omega_{di})}{\omega_A^2} \right]^{1/2} = \frac{1}{8} [\lambda_H + \lambda_k(\omega)] Q^{3/2} \frac{\Gamma[(Q-1)/4]}{\Gamma[(Q+5)/4]} \quad (\text{IV.14})$$

The functional for the energetic particles involves the parallel and perpendicular components of the perturbed pressure, determined via the moments of the perturbed distribution function, Eq. (IV.7). The derivation of the gyrokinetic equation for the perturbed distribution function for $m^0 = 1$ modes is made tedious by the fact that one cannot use the ordering $k_\perp \gg 1/r$ (i.e., the standard [80]-[81] eikonal representation) in the “external region”. This derivation is reported elsewhere [82]; here we report the result:

$$\tilde{f}_h(\mathbf{r}, \mathbf{v}) = - \vec{\xi} \cdot \nabla F_h + i m_h (\omega - \omega_{*h}) \frac{\partial F_h}{\partial \mathcal{E}} \int_{-\infty}^t dt' \left(\frac{v_\perp^2}{2} + v_\parallel^2 \right) \bar{\kappa} \cdot \vec{\xi} \quad (\text{IV.15})$$

In deriving this expression (\tilde{f}_h is actually the gyrophase average of the perturbed distribution function), the ideal MHD relation, $\mathbf{E} - i\omega \vec{\xi} \times \mathbf{B}/c = 0$, was used, as well as the approximate [79] relationship, $\nabla \cdot \vec{\xi}_\perp + 2 \bar{\kappa} \cdot \vec{\xi}_\perp = 0$. Contributions from $\tilde{B}_\parallel \sim \tilde{B}_\perp$ as well as FLR effects ($k_\perp \rho_h \sim \rho_h/r_s \ll 1$ in the exterior region) were neglected. The equilibrium distribution function F_h is a function of the total energy, $\mathcal{E} = m_h v^2/2$, and

of the toroidal component of the canonical angular momentum (a constant of the motion since the toroidal angle ζ is an ignorable coordinate), $P_\zeta = m_h v_\zeta - q\psi_0/c$. Here ψ_0 is the equilibrium poloidal flux, $\mathbf{B} = \hat{e}_\zeta B_\zeta + \hat{e}_\zeta \times \nabla\psi_0$. The diamagnetic frequency is expressed as:

$$\omega_{*h} = \frac{n^0}{R} \frac{\partial F_h / \partial P_\zeta}{\partial F_h / \partial \mathcal{E}} \quad (\text{IV.16})$$

The term involving the orbit integral in Eq. (IV.15) is of order $(\xi_\perp F_h / R) (\omega - \omega_{*h}) / (\omega - \hat{\omega}_h)$, where $\hat{\omega}_h$ is a characteristic frequency of the energetic particle orbit (i.e., the transit frequency, ω_{th} , of a circulating particle or the bounce frequency, ω_{bh} , of a trapped particle). One generally orders:

$$\omega_{th} > \omega_{bh} \gg \omega_{*h} > \omega_{Dh} \geq |\omega| \quad (\text{IV.17})$$

where $\omega_{Dh} \equiv (n^0 q / \Omega_h r R)(v_\parallel^2 + v_\perp^2 / 2)$ is the precession frequency engendered by the curvature and grad-B drifts of the particle guiding center. Then, as a consequence of this ordering, it is easy to see that the lowest order contribution from the circulating particles is “adiabatic”:

$$\tilde{f}_{h,c} \approx - \vec{\xi} \cdot \nabla F_{h,c} \quad (\text{IV.18})$$

in that it yields no contributions that are out of phase with the displacement (the perturbed pressure tensor contribution from the circulating particles has the form $\tilde{p}_{h,c} \approx - \vec{\xi} \cdot \nabla p_{h,c}$ and looks identical to the contribution from the core plasma).

Trapped particles, on the other hand, contribute non-negligibly from the orbit integral. One can adopt a representation for $X \equiv (v_\parallel^2 + v_\perp^2 / 2) \vec{\kappa} \cdot \vec{\xi}$ in terms of the periodicity of

the trapped particle orbit [83]-[84]

$$X(\mathbf{r}, \mathbf{v}, t) = \exp \left[in^0(\zeta - q\theta) - i \left(\omega - \omega_{Dh}^{(0)} \right) t \right] \sum_{m=-\infty}^{\infty} X_m(r) \exp(im\omega_{bh}t) \quad (\text{IV.19})$$

where the time variable t can also be written in terms of the particle trajectory along the magnetic field line: $dt = d\theta/v_{\parallel}(\theta)$. The phase factor shown in Eq. (IV.19) includes $n^0(\zeta - q\theta)$ which plays the role of a perpendicular wavenumber; it is the dependence of X along the magnetic field line which is decomposed in terms of basis functions. The bounce averaged precession drift frequency is defined as:

$$\omega_{Dh}^{(0)} \equiv \frac{\int_{-\theta_0}^{\theta_0} d\theta \omega_{Dh}(\theta)/|v_{\parallel}(\theta)|}{\int_{-\theta_0}^{\theta_0} d\theta/|v_{\parallel}(\theta)|} \quad (\text{IV.20})$$

In expression (IV.19), we have introduced the turning angle, θ_0 , where $v_{\parallel}(\theta = \theta_0) = 0$ and we have neglected contributions from the banana radius of the trapped particle orbits. The expressions corresponding to (IV.19) with finite banana radius can be found, e.g. in Refs. [85]-[87]. Then, the perturbed distribution of energetic trapped particles reads:

$$\begin{aligned} \tilde{f}_{h,t} = & - \vec{\xi} \cdot \nabla F_{h,t} - m_h \frac{\partial F_{h,t}}{\partial \mathcal{E}} \sum_{m=-\infty}^{\infty} X_m(r) \frac{\omega - \omega_{*h}}{\omega - \omega_{Dh}^{(0)} - m\omega_{bh}} \\ & \exp \left[in^0(\zeta - q\theta) - i \left(\omega - \omega_{Dh}^{(0)} + m\omega_{bh} \right) t \right] \end{aligned} \quad (\text{IV.21})$$

In the limit of large bounce frequency only the $m = 0$ term contributes. Note that an analogous form can formally be derived for circulating particles except that $m\omega_{bh} \rightarrow (m + S)\omega_{th}$ where $S \approx 1 - q(r)$. It is because of the finite magnetic shear that the “non-adiabatic” contribution of circulating particles is of order $(\omega - \omega_{*h})/S\omega_{th} \ll 1$. Evaluating X_0 is straightforward:

$$X_0 = \frac{\int_{-\theta_0}^{\theta_0} \frac{d\theta}{|v_{\parallel}(\theta)|} \frac{2\mathcal{E}}{m_h} \left(1 - \frac{\Lambda}{2h}\right) \exp[-in^0(\zeta - q\theta)] (\vec{\kappa} \cdot \vec{\xi})}{\int_{-\theta_0}^{\theta_0} d\theta/|v_{\parallel}(\theta)|} \quad (\text{IV.22})$$

where we introduce the well-known [84] pitch angle coordinate $\Lambda \equiv \mu B_0 / \mathcal{E} = v_\perp^2 B_0 / v^2 B$, as well as $h(r, \theta) \equiv B_0 / B$; here B_0 is the reference value of the magnetic field at $\theta = 0$ (the outer point of the mid-plane). In terms of Λ , phase space is defined as follows: $0 \leq \Lambda \leq h_{min}$ is occupied by circulating particles, while $h_{min} \leq \Lambda \leq h_{max}$ is occupied by trapped particles. For low- β equilibria $h(r, \theta) = 1 + (r/R) \cos(\theta)$, thus $h_{min} = 1 - r/R$ and $h_{max} = 1 + r/R$. Since X_0 is already of order ϵ , one can take $1 - \Lambda/2h \approx 1/2$ under the integral and, using $\vec{\kappa} \approx (1/R)(-\hat{e}_r \cos \theta + \hat{e}_\theta \sin \theta)$, obtain [88]:

$$X_0 \approx -(\mathcal{E}/Rm_h)(\cos q\theta)^{(0)} \bar{\xi}_r(r) \quad (\text{IV.23})$$

where $\bar{\xi}_r \equiv \xi_r(\mathbf{r}, t) \exp[i\omega t - i(n^0 \zeta - m^0 \theta)]$, with $m^0 = n^0 = 1$. The lowest order relation $\nabla_\perp \cdot \vec{\xi} \sim \epsilon \xi_\perp \Rightarrow \xi_\theta \approx -i\xi_r$ has also been used. Hence we finally obtain [88]:

$$\tilde{f}_h \approx -\vec{\xi} \cdot \nabla F_h + \mathcal{E} \frac{\partial F_{h,t}}{\partial \mathcal{E}} \frac{\omega - \omega_{*h}}{\omega - \omega_{Dh}^{(0)}} (\cos q\theta)^{(0)} \frac{\xi_r}{R} \quad (\text{IV.24})$$

The subscript t in the second term indicates that only the trapped fraction of energetic particles is to be considered, while the superscript (0) denotes a bounce average, cf. Eq. (IV.20). Note the importance of Eq. (IV.17): it is precisely the fact that the particles precess (ω_{Dh}) faster than the mode rotates that sets them apart as a species. This precession drift dominates their response to the perturbation and causes them not to $\mathbf{E} \times \mathbf{B}$ drift with the rest of the plasma. An alternate description of the unique role played by energetic particles has been given by Porcelli [89]: these particles conserve the third adiabatic invariant (the poloidal flux passing through a surface mapped out by the precessing guiding centers) when they are “fast enough” compared to the mode phase velocity. They react to the perturbation in such as fashion as to conserve this linked flux, and in doing

so exert a stabilizing influence (provided a set of conditions on the q -profile and on the bounce-averaged precession drift frequency is met) on the mode.

From Eqs. (IV.-7) and (IV.13) and the definition of the magnetic curvature vector, $\vec{\kappa}$, we see that the energetic particles to the functional λ_k through a term of the type $\oint d\theta(\sin \theta + \alpha \cos \theta)(\text{something})$. Thus, the integral vanishes whenever that "something" is θ -independent. For example, the "adiabatic" piece, $-\vec{\xi} \cdot \nabla F_h$, does not contribute if the equilibrium distribution function of the energetic particles is isotropic in velocity space. When it does contribute, it generally does so in a destabilizing manner, as can be seen from:

$$\lambda_k^{ad} = - \frac{4\pi^2 i m^0}{(B_\theta^2 s)_{r_s}} \int_0^{r_s} dr r^2 \int_{-\pi}^{\pi} \frac{d\theta}{2\pi} \exp(i\theta) \left(\frac{\cos \theta}{r} \frac{\partial}{\partial \theta} + \sin \theta \frac{\partial}{\partial r} \right) \left[\frac{\partial p_{\perp h}(r, \theta)}{\partial r} \exp(-i\theta) \right] \quad (\text{IV.25})$$

for the case of a population of deeply trapped particles ($0 \leq |\theta| \leq \theta_0$ where $\theta_0 < \pi/2$).

The $\sin \theta$ term drops out, being odd in θ , while an integration by parts yields:

$$\lambda_k^{ad} = - \frac{4\pi m^0}{(B_\theta^2 s)_{r_s}} \int_0^{r_s} dr r \int_0^{\theta_0} d\theta \cos \theta \frac{\partial p_{\perp h}}{\partial r} \quad (\text{IV.26})$$

which clearly is a positive (destabilizing) quantity for pressure profiles that are peaked at the center.

From Eq. (IV.7) (IV.13) and (IV.24), one is led to conclude that the expression for λ_k depends principally on the mode frequency (relative to characteristic values of $\omega_{Dh}^{(0)}$ and/or ω_{*h}), the degree of anisotropy of the equilibrium velocity space distribution function, the degree of peakedness of the density and/or temperature profile, and the q -profile (cf. $(\cos q\theta)^{(0)}$ in Eq. (IV.24)). This is indeed true, as will be discussed in the

next sub-section, however our experience with models used for several experiments seems to indicate a certain universality in the curve $\lambda_k(\omega)$, given a real eigenfrequency; this points out that some of these dependences may be weak. As examples, we offer in Figs. 4 and 5 respectively, plots of $\lambda_k(\omega)$ appropriate for the experiments in JET [60]-62] and for a slowing-down distribution of α -particles produced by fusion reactions in the planned IGNITOR [90] experiment. In the former case, the equilibrium distribution function is highly anisotropic (being comprised almost exclusively of trapped particles with turning points at $\theta_0 = \pm\pi/2$). In the latter case, the distribution function is perfectly isotropic. Yet the two graphs are strikingly similar: $Im(\lambda_k)$ is negative definite (the sign is the appropriate one for positive dissipation, $\nu > 0$ in Eq. (IV.2), necessary to stabilize the “sawtooth” and destabilize the “fishbone”) while $Re(\lambda_k)$ is negative at low frequency and positive at high frequency. With this information we can glean some salient features of the effects of energetic particles on $m^0 = 1$ modes. Let us examine Eq. (IV.14) in the $|Q| \gg 1$ limit, assuming that $|\lambda_k| < \lambda_H$. Then, using the large argument relationship between the two gamma functions, cf. [91], we obtain:

$$\left[-\frac{\omega(\omega - \omega_{di})}{\omega_A^2} \right]^{1/2} \approx [\lambda_H + \lambda_k(\omega)] \left[1 - \frac{5}{4} \frac{i\epsilon_\eta \omega_A^3}{\omega(\omega - \omega_{di})(\omega - \hat{\omega}_{*e})} \right] \quad (IV.27)$$

after using the definition for Q , Eq. (II.21). Proceeding in the same manner as we did in solving Eq. (IV.1), we obtain the two solutions (in the regime where $\lambda_H < \omega_{di}/2\omega_A$):

$$\omega \approx \frac{\omega_A^2}{\omega_{di}} \left[\lambda_H + \lambda_k(\omega = \lambda_H^2 \omega_A^2 / \omega_{di}) \right]^2 + \frac{5}{2} \frac{i\epsilon_\eta \omega_A^3}{|\omega_{di} \hat{\omega}_{*e}|} \quad (IV.28 - a)$$

$$\omega \approx \omega_{di} - \frac{\omega_A^2}{\omega_{di}} \left[\lambda_H + \lambda_k(\omega = \omega_{di}) \right]^2 - \frac{5}{2} \frac{i\epsilon_\eta \omega_A^3}{\omega_{di}(\omega_{di} - \hat{\omega}_{*e})} \quad (IV.28 - b)$$

Remembering that $[\lambda_H + \lambda_k]^2 = (\lambda_H + Re\lambda_k)^2 - (Im\lambda_k)^2 + 2i(\lambda_H + Re\lambda_k)(Im\lambda_k)$, it is obvious that Eq. (IV.2) and (IV.28) are analogous provided that $(Im\lambda_k)(\lambda_H + Re\lambda_k) < 0$,

which is the case for low the values of the parameter $\omega/\bar{\omega}_{Dh}$ considered here (as shown in Figs. 4 and 5). Thus, the first root (the resistive internal kink) tends to be stabilized by the “resonant” coupling to the energetic particles (represented by $Im\lambda_k$), while the second is destabilized by it.

On the other hand, an “ideal-like” instability is obtained from Eq. (IV.27) in the limit $\lambda_H > \omega_{di}/2\omega_A$:

$$\omega \approx \frac{1}{2}\omega_{di} + i\omega_A \left\{ [\lambda_H + \lambda_k(\omega = \omega_{di}/2)]^2 - \left(\frac{\omega_{di}}{2\omega_A}\right)^2 \right\}^{1/2} \quad (\text{IV.29})$$

Since $Re\lambda_k(\omega \leq \omega_{di} \ll \bar{\omega}_{Dh})$ is negative, the introduction of energetic particles tends to similarly stabilize the ideal internal kink. Here we use $\bar{\omega}_{Dh} \equiv 1.2\mathcal{E}_h(1+2s(r_s))/(m_h\Omega_h Rr_s)$ as a representative value of the bounce averaged precession frequency.

Considerations of this type were responsible for the initial models [92]-[97] that successfully explained the physics responsible for the stabilization of sawteeth in existing experiments [60]-[64], and were used to predict [88] similar beneficial effects from fusion α -particles in future ignited toroidal experiments. Since this is by now considered an important success, both theoretical and experimental, in the confinement of particles and energy within the central portion of the plasma, we address the question of sawtooth stabilization in further detail in the following paragraphs. We will return to the question of fishbone oscillations (whose experimental observation and theoretical modelling actually preceded that of sawtooth suppression) in the final sub-section.

IV.2 Sawtooth stabilization

The basic features of the stabilization have been presented above. Here, we begin by addressing a crucial detail: the stabilization of resistive internal kinks. For a given value of

$\lambda_H > 0$, the introduction of energetic particles stabilizes the ideal internal kink as soon as $\lambda_H + \text{Re}\lambda_k < \omega_{di}/2\omega_A$, cf. Eq. (IV.29). The resistive internal kink, which remains unstable once that threshold is crossed, has its growth rate decreased by the dissipation due to mode-particle resonance, represented by the combination $2i(\omega_A^2/\omega_{di})(\lambda_H + \text{Re}\lambda_k) (\text{Im}\lambda_k) < 0$. At the same time, the real part of the mode frequency decreases like $(\lambda_H + \text{Re}\lambda_k)^2 < \lambda_H^2$ (for the purpose of illustration, we envision a process in which the density of energetic particles is increased gradually, $\lambda_k \propto n_h$, and the mode adjusts its behavior accordingly). From Figs. 4-5, we see that, as $\omega \rightarrow 0$, $\text{Im}\lambda_k$ also vanishes. Of course, Eq. (IV.28) is no longer valid, so that Eq. (IV.14) must be considered. As originally shown in Ref. [5], the point $\lambda_H + \lambda_k = 0$ corresponds to the dispersion relation $Q = 1$, with a purely growing mode, $\omega \approx i\epsilon_\eta\omega_A^2/|\omega_{di}\hat{\omega}_{*e}|$. Hence, one must ask: what happens when $\omega \rightarrow 0$? Unless the real part of λ_k remains finite (and negative), the stabilization process “stalls” and resistive internal kinks cannot be completely stabilized. That was the conclusion reached in Refs. [92], [94]-[97], where the expression for the energetic particle functional was specifically derived for a population of deeply trapped particles, $F_h \propto \delta(\Lambda - \Lambda_0)$ with $\Lambda_0 \approx 1$, and was of the form [98]:

$$\lambda_k(\omega) = \beta_{ph} \frac{\omega}{\bar{\omega}_{Dh}} \ln \left(1 - \frac{\bar{\omega}_{Dh}}{\omega} \right) \quad (\text{IV.30})$$

(this expression obviously vanishes at zero frequency). As a consequence, this particular form for λ_k caused the authors of Ref. [95] to comment that in order “to achieve stabilization with trapped particles, the kink mode must be above its threshold” ($\lambda_H > \omega_{di}/2\omega_A$ in our notation).

However, as indicated in Figs. 4-5, there exists the probability that the real part of

the energetic particle functional is actually negative and finite as $\omega \rightarrow 0$. The expression for the energetic particle functional, in the limit of vanishing mode frequency, is [93]:

$$\begin{aligned} \lambda_k(\omega = 0) = & \frac{4\pi^3}{(B_p^2 s)_{r_s}} \left(\frac{r_s}{R}\right) \left(\frac{2}{m_h}\right)^{3/2} \int_0^1 d\hat{r} \hat{r} \int_{h_{min}}^{h_{max}} d\Lambda (\sigma \Lambda) \\ & \times \left(\frac{I_q^2}{I_d} - I_c\right) \int_0^\infty d\mathcal{E} \mathcal{E}^{3/2} \frac{\partial F_h}{\partial \hat{r}} \end{aligned} \quad (\text{IV.31})$$

where we correct for an improper factor of $1/q$ (due to an erroneous definition of ω_{*h}) as well as a misprint in the corresponding formula in Ref. [93]. Here $\hat{r} \equiv r/r_s$, $\sigma \equiv \int_{-\theta_0}^{\theta_0} (d\theta/2\pi)[1 - \Lambda/h(r, \theta)]^{1/2}$, $I_c \equiv (\cos \theta)^{(0)}$, $I_q \equiv (\cos q\theta)^{(0)}$, $I_d \equiv (\cos \theta + s\theta \sin \theta)^{(0)}$, $s(r) = rdq/dr$, and θ_0 is the turning point of a given trapped particle (i.e., a function of the pitch angle). This expression has been obtained from (IV.13) by making some simplifying assumptions, most notably $1 - \Lambda/2h \approx 1/2$, and holds for a species of energetic particles that is wholly trapped: $F_h = 0$ for $\Lambda \leq h_{min} \sim 1 - r/R$. The contribution from the “adiabatic” portion of the energetic particle response is indicated by the factor I_c , while that from the “non-adiabatic” response is indicated by $I_q^2/I_d = [(\cos q\theta)^{(0)}]^2 (\mathcal{E}/\mathcal{E}_h)(r_s/R)(\omega_{*h}/\omega_{Dh}^{(0)})$, where \mathcal{E}_h is the maximum particle energy. It is obvious that the two contributions tend to oppose each other. Furthermore, if we assume that $|q(r) - 1|$ is small within the $r \leq r_s$ region, we can expand this quantity in a Taylor series and obtain:

$$\lambda_k \propto (I_q^2 - I_c I_d) \frac{\partial F_h}{\partial r} \approx [2(1 - q(r)) - s(r)] (\theta \sin \theta)^{(0)} \frac{\partial F_h}{\partial r} \quad (\text{IV.32})$$

Thus, in this case $\lambda_k(\omega = 0)$ is of order $1 - q_0$ as originally stated in Ref. [99]. For parabolic q -profiles, $\lambda_k \propto 2[q_0/q(r) - q(r)] (\theta \sin \theta)^{(0)} \partial F_h / \partial r$ and is negative definite for trapped particles with a (perpendicular) pressure profile that is strongly peaked in the center. Note also that $\lambda_k(\omega = 0)$ is independent of the particle charge. Hence, energetic electrons,

due e.g., to ECH, could be candidates for stabilization of resistive internal kinks (G. E. Guest [private communication, 1988] and [97]). Curves of marginal stability, $Im(\omega) = 0$, have been presented in a number of references (e.g., [88], [93], [95]-[97]), generally in either $\beta_p - \beta_{ph}$ or $\omega_{di} - \beta_{ph}$ parameter space. Here, we choose to reproduce one such figure, from Ref. [88], which shows the dependence on the parameter $\epsilon_s = r_s/R$. This figure is Fig. 6 in the present paper.

Note that some form of dissipation is necessary to counter the effect of resistivity (or, in its absence, electron Landau damping [42], [51], [54]) and, if this dissipation is to come from a resonance between the mode and energetic particles, then one necessarily needs $Re(\omega)/\omega_{Dh}^{(0)} > 0$. Since the sign of $Re(\omega)$ is generally the same as that of $(\lambda_H + Re\lambda_k)\omega_{di}$, we see that the mode resonates with deeply trapped energetic ions for positive $\lambda_H + Re\lambda_k$ and trapped electrons otherwise. The word “deeply” is used here to remind the reader that the drift-reversal boundary (the point in pitch angle space where $\omega_{Dh}^{(0)}$ changes sign) occurs near the boundary between trapped and circulating particles (cf. Fig. 9 in Ref. [84] and Fig. 3 in Ref. [79]). The existence of the drift-reversal is well-known and has been fully taken into account in evaluations of the energetic particle functional, e.g., in Refs. [88] and [93], contrary to assertions made recently [100]. If parameters are such that a resonant interaction between the wave and the energetic particles is either absent or insufficient, stabilization may be possible through other viscous-like processes (e.g., ion-ion collisional viscosity, cf. [53]).

From a practical point of view, the ratio r_s/R is of crucial importance to the stabilization process. The parameter controlling the instability (say, in the limit $\epsilon_\eta \rightarrow 0$) is

$\lambda_H \approx (3\pi/2) (r_s/R)^2 (\beta_p^2 - \beta_{pc}^2)$. The parameter controlling stabilization on the other hand is $\lambda_{k0} \equiv \beta_{p\alpha} (r_s/R)^{3/2}$, for the case of Fig. 6. The two poloidal betas are [10]:

$$\beta_p \equiv - \frac{8\pi}{B_p^2(r_s)} \int_0^{r_s} dr \left(\frac{r}{r_s} \right)^2 \frac{dp_c}{dr} \quad (\text{IV.33 - a})$$

and [87]:

$$\beta_{p\alpha} \equiv - \frac{8\pi}{B_p^2(r_s)} \int_0^{r_s} dr \left(\frac{r}{r_s} \right)^{3/2} \frac{dp_\alpha}{dr} \quad (\text{IV.33 - b})$$

From the properties of $\lambda_k(\omega)$, cf. Fig. 4-5, there exist maximum values of λ_H and λ_{k0} for which stabilization is possible. They are determined by a pair of equations, e.g., Eq. (26)-(27) in Ref. [88] for the case of vanishing resistivity. For instance, $\max(\lambda_{k0})$ occurs where the marginal stability curve crosses the $\lambda_H = 0$ axis, and corresponds to $\text{Re}\lambda_k(\omega) = 0$. This determines $\omega/\bar{\omega}_{D\alpha}$, (cf. Fig. 6, where $\bar{\omega}_{D\alpha}$ is defined) which, in turn, determines λ_{k0} from the second of the pair of equations. The existence of these two “maximal” points immediately tells one that $(\Delta\beta_p^2)_{\max} \propto (R/r_s)^2$ and $\beta_{p\alpha}^{\max} \propto (R/r_s)^{3/2}$, which accounts for the shrinkage of the stable region. This makes experiments with “large” inverse aspect ratio, $r_s/R \geq 0.5$, undesirable from the point of view of stability of $m^0 = 1$ modes, as was mentioned in Ref. [100]. Some corroboration of this point comes from experiments in JET. As reported in [62] and [101], the interval of sawtooth-free operation decreased with increasing inversion radius (which is presumably coincident with $q(r = r_s) = 1$). Also of note from these experiments is the fact that the longest interval occurred for the case where the ICRH was positioned at the center of the plasma column, which probably maximized $\partial p_h / \partial r$.

The scaling $\lambda_{k0} \propto (r_s/R)^{3/2} \beta_{p\alpha}$ comes about from two sources: (i) a factor of r_s/R coming from the magnetic curvature κ , and (ii) a factor of $(r_s/R)^{1/2}$ that reflects the

fact that only trapped particles contribute to the stabilization. Remember also that, for isotropic equilibrium distribution functions, only the “non adiabatic” part of the perturbed response contributes to λ_k . On the other hand, if all the energetic particles are trapped, such as occurs for highly anisotropic ion distribution functions produced by ICRH, the natural scaling is $\lambda_{k0} \propto (r_s/R)\beta_{ph}$, where [93]:

$$\beta_{ph} \equiv - \frac{8\pi}{B_p^2(r_s)} \int_0^{r_s} dr \frac{r^{3/2}}{r_s^2} \frac{\partial}{\partial r} \left(r^{1/2} p_{\perp h} \right) \quad (\text{IV.34})$$

In either case ($\beta_{p\alpha}$ or β_{ph}) the poloidal beta denotes the total (trapped + circulating) energy content of the species doing the stabilization.

Just like there exists a maximum value of λ_H at which stabilization is possible, there also exists a maximum value of $\omega_{di}/\bar{\omega}_{Dh}$. This has been addressed and shown, first in Refs. [96]-[97], and then in Ref. [88]. This is not surprising in retrospect, as it is precisely the smallness in the parameter $\omega/\bar{\omega}_{Dh} \leq \omega_{di}/\bar{\omega}_{Dh}$ that makes these particles “energetic” and, therefore stabilizing. It is instructive to look at a “cartoon” of the stabilization process in the case of vanishing resistivity, $\epsilon_\eta = 0$. The dispersion relation is given by Eq. (IV.27) with unstable root

$$\begin{aligned} \omega \approx \frac{1}{2}\omega_{di} + i \left[\omega_A^2 (\lambda_H + Re\lambda_k)^2 - \frac{1}{4}\omega_{di}^2 \right]^{1/2} \\ + 2i \left(\frac{\omega_A^2}{\omega_{di}} \right) (\lambda_H + Re\lambda_k)(Im\lambda_k) \end{aligned} \quad (\text{IV.35})$$

with λ_k evaluated at $\omega = \omega_{di}/2$ and where we assumed that $Im\lambda_k$ is small. Hence, as the density of energetic particles (or, equivalently, β_{ph}) is increased, the growth rate decreases through a combination of smaller free energy, $\lambda_H + Re\lambda_k$, and dissipation due to wave-particle resonance, $Im\lambda_k < 0$. When the free energy drops below the value necessary

to overcome FLR stabilization, $\omega_{di}/2\omega_A$, the ideal internal kink becomes stable, and the other root is resonantly destabilized

$$\omega \approx \omega_{di} - \left(\frac{\omega_A^2}{\omega_{di}} \right) [(\lambda_H + Re\lambda_k)^2 + 2i(\lambda_H + Re\lambda_k)(Im\lambda_k)] \quad (\text{IV.36})$$

with λ_k evaluated at $\omega = \omega_{di}$. This is the instability of the “fishbone”, which we will consider in the next sub-section. This unstable mode persists until the zero free energy point, $\lambda_H + Re\lambda_k = 0$, is reached, where growth stops.

These last remarks have focussed on the stabilization of ideal modes ($\epsilon_\eta = 0$ and no electron Landau damping). They carry over to resistive internal modes as well. A stable region of finite size exists in parameter space for resistive modes, as can be seen in Refs. [93] and [101]. Also, the appearance of the fishbone instability on the heels of the stabilized resistive internal kink was briefly mentioned in [94]. Note that a finite region of stability exists only if one or both of the following conditions is satisfied: (i) $\omega_{di} \neq 0$, (ii) $\lambda_k(\omega = 0) \neq 0$. The latter corresponds to having $1 - q_0 > \epsilon_s \equiv r_s/R$ for anisotropic particles. Models that did not include either of these effects, e.g., [102], necessarily missed this stability window.

Further work is now underway to determine the effect of finite Larmor radius (i.e., FLR of the core plasma ions within the singular layer) on this stabilization mechanism. As discussed in the previous section, FLR tends to worsen stability and, hence, will make stabilization by energetic particles harder to achieve. This was noted in a preliminary fashion in Ref. [88] and has been fully discussed in [103]: energetic particles interact resonantly with a discrete spectrum of resistively damped Alfvén eigenmodes. This wave particle resonance can destabilize these eigenmodes.

The existence of a right-hand boundary to the stable region, shown in Fig. 6, namely the line connecting the point $(\Delta\beta_p^2)_{max}$ to the point $\beta_{p\alpha}^{max}$ signals the appearance of a new instability with higher frequency, $Re(\omega) \geq \bar{\omega}_{Dh}$. We have indicated how the point of marginal stability $\beta_{p\alpha}^{max}$ corresponds to a frequency $\omega \approx \bar{\omega}_{Dh}$ such that $Re\lambda_k = 0$, cf. Figs. 4-5. Past this point, the combination $\lambda_H + Re\lambda_k$ necessarily is positive and this new instability is supported by the energetic trapped particles, both in its resonant form (near the marginal stability boundary) and in its fluid-like form (far away from it). This trapped particle branch was discovered by the authors of Ref. [98], in connection with the theory of fishbone oscillations.

One last detail worth mentioning is the behavior of the instability in the region immediately above the apex of the stable region. Near this apex there exists a small but finite region in parameter space, where two unstable modes co-exist. One mode corresponds to the lower frequency branch (for which $\omega = \omega_{di}$ at $\lambda_H = \beta_{ph} = 0$), and the other to the high frequency branch ($\omega \approx \bar{\omega}_{Dh}$ at $\beta_{ph} = \beta_{ph}^{max}$). This region has been identified numerically in repeated occasions, and can be most easily found in cases where $\omega_{di} = 0$ (cf. Fig. 4 of Ref. [88]) or where the energetic particle equilibrium distribution function is highly anisotropic. This result helps establish the rather important property that the high frequency and low frequency unstable roots are indeed distinct modes. With the advent of the more recent work [103] on FLR effects on this problem of stabilization, this domain of multiple unstable roots has been enlarged by the appearance of the aforementioned Alfvén spectrum, destabilized by resonant interactions (cf. Fig. 5 of Ref. [103]).

Finally, the existence of an alternate model for the sawtooth stabilization process

ought to be mentioned. As originally proposed [104], this model ascribed the stabilization to direct ponderomotive effects from the ICRH wave field. It failed one crucial experimental test, that of the time delay (approximately 80 – 100 msec in JET [105]) between ICRH switch-off and the first sawtooth crash. This time delay is commensurate with the slowing-down time of an energetic ion [101], which tends to favor the model discussed so far. The ponderomotive force model has since been modified [106] to account for this time delay. In the modified model, Alfvén ion cyclotron waves, generated by the anisotropic energetic ion distribution, have a ponderomotive force that causes the stabilization. The time delay is explained in terms of the time required to isotropise the distribution function. Thus, in final analysis, the energetic particles are again the agents for stabilization though they might use more than one “channel” to do the job.

IV.3 Excitation of fishbone oscillation bursts

As mentioned at the beginning of this section, work on energetic particle effects on $m^0 = 1$ modes actually began with the discovery [69]-[72] of so-called “fishbone oscillation bursts”. The two models, that arose initially [98] and [107] to explain these bursts, had a common main feature: an marginally stable mode is destabilized by a resonance with trapped energetic ions; the resonance is of the form $\omega - \omega_{Dh}^{(0)}(\mathcal{E}, \Lambda, r) = 0$. Where they differed, however, was in the identification of the mode involved. Coppi and Porcelli [107] identified it as being the higher frequency branch of the already existing pair of modes from the fluid response of the core plasma. Chen, White, and Rosenbluth [98] instead ascribed it to a new branch, created by the energetic trapped particles. As we have seen in the paragraph above, both interpretations are correct. It can be argued that

experiments were probably operating in the region of parameter space just above the apex of the marginal stability curve, cf. Fig. 6. Indeed, if $\omega_{di} \approx \bar{\omega}_{Dh}$ as occurred in the experiments which detected the fishbone oscillation bursts in PDX [69]-[71] and DIII-D [73], the stable region disappears altogether, and the two roots connect into one continuous instability as β_{ph} is varied. In passing, we mention that the models of Refs. [98] and [107] were further developed and refined in [108] and [79], respectively. The small stabilizing effect of resistivity on the trapped particle induced fishbone oscillation of Ref. [98] was first presented in Ref. [109]. As discussed in the latter part of the previous sub-section, the fishbone instability arises near the marginal stability limit of $m^0 = 1$ modes, and appears as a resonantly driven version of either a core plasma mode ($\omega \approx \omega_{di}$) or a trapped particle mode ($\omega \approx \bar{\omega}_{Dh}$). A pictorial representation of this, drawn from Ref. [88], is shown in Fig. 7.

Perhaps the most lucid analysis of the relationship between the two fishbone roots can be found in [96], where the nomenclature ‘‘Coppi-Porcelli fishbone’’ and ‘‘Chen-White-Rosenbluth’’ fishbone was coined. By specializing to a strongly anisotropic, slowing-down, distribution of energetic particles

$$F_h = \frac{C_h \delta(\Lambda - \Lambda_0)}{(\mathcal{E}^{3/2} + \mathcal{E}_c^{3/2})} \quad (\text{IV.37})$$

with $\Lambda_0 \approx 1$, and thereby obtaining the functional [96], [98], [104]:

$$\lambda_k(\omega) = \tilde{\beta}_{ph} \frac{\omega}{\bar{\omega}_{Dh}} \ln \left(1 - \frac{\bar{\omega}_{Dh}}{\omega} \right) \quad (\text{IV.38})$$

in the limit where $1 - q_0$ is negligible, the authors of Ref. [96] were able to show how the marginal stability properties of the two roots were related. Here $\tilde{\beta}_{ph}$ is a quantity of the

order of β_{ph} whose definition can be found in Eq. (6) of Ref. [96]. From Eq. (IV.38), it is obvious that one condition for marginal stability is $\omega = \bar{\omega}_{Dh}/2$ when $\omega_{di} = \lambda_H = 0$. This can be seen from the dispersion relation which, in the limit of vanishing resistivity, can be cast in the form

$$\sqrt{\omega(\omega - \omega_{di})} = -i[\lambda_H + \lambda_k(\omega)]\omega_A \quad (\text{IV.39})$$

The corresponding value of $\tilde{\beta}_{ph}$ is [98]: $\tilde{\beta}_{ph} = \bar{\omega}_{Dh}/\pi\omega_A$. If $\omega_{di}/\bar{\omega}_{Dh}$ and λ_H are both small positive quantities, marginal stability occurs for:

$$\tilde{\beta}_{ph} = \frac{\bar{\omega}_{Dh}}{\pi\omega_A} \left(1 - \frac{\omega_{di}}{\bar{\omega}_{Dh}} \right) - \lambda_H \quad (\text{IV.40})$$

with a mode frequency $\omega \approx \omega_{di} + (\pi/2)\lambda_H\omega_A$. Hence, the addition of either finite ion diamagnetic frequency or free energy makes this branch more unstable [96] (the critical value of $\tilde{\beta}_{ph}$ is encountered sooner).

This has been a description of the marginal stability of the high frequency (Chen-White-Rosenbluth) fishbone. The other root, the low frequency (Coppi-Porcelli) fishbone is marginally stable for [96]:

$$\tilde{\beta}_{ph} = \frac{\bar{\omega}_{Dh}\lambda_H}{\omega_{di} \ln(\bar{\omega}_{Dh}/\omega_{di} - 1)} \quad (\text{IV.41})$$

for small λ_H and $\omega_{di}/\bar{\omega}_{Dh}$, which shows the opposite trend with λ_H (also a destabilizing trend, as now more particles are needed to stabilize the mode). In both cases, the trend agrees with the complete numerical results presented, e.g., in Figs. 6-7. The decrease in $\tilde{\beta}_{ph}$ with larger ω_{di} is simply a consequence of energetic particles no longer having a “fast” precession frequency compared to the benchmark frequency of the core plasma.

Both models [98] and [107] also include a nonlinear cycle in which energetic particles generate the fishbone instability, are in turn scattered out of the region of resonant interaction, thereby lowering β_{ph} to values below that needed for instability and terminating the fishbone burst [79], [98], [108]. As the density of energetic particles is replenished, e.g. by neutral beams, the fishbone is again triggered, and the cycle is repeated. This process has been invoked [110] as a mechanism for plasma self-purification in ignited experiments. Slowed-down α -particles, with energies $\mathcal{E} = 300 - 400$ KeV, can resonate with $\omega \approx \omega_{di}$ modes and be transported out of the central plasma core. This would mitigate the problem of the “poisoning” of the plasma by Helium ash (thermalized α -particles) which dilutes the $D - T$ fuel.

Where these models are deficient, however, is in describing “fishbone – like” oscillations observed in PBX [111]-[112] and in DIII-D [113] with tangential neutral beam injection. Since both models require a population of energetic trapped particles, experiments which produce mostly passing (“circulating”) particles present a challenge to these models. In the DIII-D experiment it was deemed [W. Heidbrink, private communication, 1990] that few, if any, trapped particles were generated within the $q = 1$ radius. Thus, excitation of these “fishbone – like” oscillations likely requires an alternate mechanism, possibly a toroidal resonance with transiting particles such as that described in Ref. [114].

V. Alternate models for sawteeth and discussion

This paper has been devoted to our present understanding of the stability properties of $m^0 = 1$ modes (ideal and resistive internal kinks) in magnetically confined toroidal plasmas. Among the topics discussed were: (a) two-fluid theory and its extension to regimes of finite electron inertia, (b) ion and electron kinetic effects in regimes of high temperature where two-fluid theory is inadequate, (c) the physics of energetic particle populations, both isotropic and anisotropic, and their role in stabilizing sawteeth and triggering fishbones.

Perhaps the most important objective of a theoretical model of the physics of these modes lies in predicting an experimentally acceptable estimate for the linear growth time of the instability; a time that is shorter than the sawtooth crash times inferred by observations. An equally important objective, one that can almost certainly be achieved only after the linear theory is complete, is the explanation of the sawtooth repetition time (this time is likely to be dynamically linked to the time scale of the relevant perturbation [115]).

Our approach has been to discuss the linear theory of $m^0 = 1$ modes in systems with finite magnetic shear. This has been motivated by measurements, e.g. on TEXTOR [22], Text [116], and JET [12], [117], which show that $q_0 < 1$ (note that other authors ascribe very low magnetic shear to JET [118] at the $q = 1$ surface, based on pellet ablation measurements while a second set of experiments [119] on Text yielded $q_0 = 1$ on the average over a sawtooth period; hence this experimental datum still needs pinning down). This in no way detracts from the importance of alternate models, each of which may in fact better explain particular features of some experiments. Perhaps the most important of these alternate models is that originally proposed by Wesson [120], in which a system with

very low shear ($s(r) \leq (r_s/R)^2$) is considered. This model was the first attempt at resolving the question of discrepancy between the linear time scale predicted by theory (the “Kadomtsev” time scale) and the much shorter time scale observed in large experiments (e.g., JET). For the case of Wesson’s model, a pressure-driven, ideal quasi-interchange mode can become unstable for arbitrarily weak pressure gradients [121], with very fast time scales [122]. Barring this possibility (see below), Table II shows that it is inherently difficult to obtain instabilities with short enough linear time scales to explain fast sawtooth crashes in large, high temperature experiments. One is left to postulate that either the fast crash is a wholly nonlinear phenomenon [15] or that the density and temperature profiles of electrons and ions are flat in the vicinity of the $q(r) = 1$ surface, thereby eliminating the beneficial effects of finite ion diamagnetic and electron drift wave frequencies. If that were the case, electron inertia is a viable dissipation mechanism, which enables the plasma and magnetic field to slide by one another, and which permits instabilities with short linear time scales, e.g., $\tau \approx (c\rho_i^2/r_s^3)^{1/3} \sim 40 \mu\text{sec}$ (cf. [40]-[41], [43]). Unfortunately, there is no experimental evidence that such a situation occurs in toroidal systems. In fact, counter-evidence exists, e.g. by pellet injection experiments [16]-[17], [123] that clearly shows examples in which peaked pressure profiles are maintained and slow down or suppress sawteeth. The question of what description is proper for the $q(r)$ -profile probably is the most important experimental datum still required for a proper theoretical description of the phenomenon. In addition to the experiments mentioned above, there exist observations [124] in JET suggesting that q_0 remains well below unity throughout the sawtooth cycle; this creates difficulty for both the quasi-interchange mode [120] that needs flat q -

profiles and for Kadomtsev-type nonlinear scenarios that result in $q_0 = 1$ after complete reconnection. Analyses of discharges in PBX-M [125] for which fishbone events were detected seem to indicate some degree of flattening of the q -profile late in the discharge, though the shear appears to remain finite at the $q = 1$ surface. On the other hand, the q -profile was also deemed to vary during the evolution of the discharge, with the profile tending to be less steep in later stages of the shot: q seemed to be nearly constant (and below unity, $q \approx 0.86$) within the inner third of the plasma column. The PBX-M experimenters [125] also raised the point that their measurements cause difficulty to both the quasi-interchange and Kadomtsev models. These experiments [125] were deemed to have exceeded the threshold for ideal internal kink instability.

Fast sawtooth crashes have also been postulated [126] to occur for non monotonic q -profiles ($q_0 \approx 1 = q(r_s)$ and $q < 1$ for $0 < r < r_s$, see also [127]-[128]; the theory of internal disruptions in plasmas with non-monotonic q -profiles was first discussed by Parail and Pereverzev [129]) that arise from gradients in the resistivity, $\nabla^2 \eta \neq 0$, which engender skin currents. Since the perturbation travels unimpeded over much of the core region (that portion where $q(r) = 1$, and where there is no restoring force from magnetic field line bending), the effective reconnection time is computed [3] using only the portion Δr where $q(r) < 1$ and the Alfvén perturbation has a finite travel time. As a consequence, reconnection and, hence, the crash occur on a much shorter time scale. There exists some corroboration from experiments for this model: in the case of some partial [130]-[131] or “giant” [132] sawteeth, inferences have been made that mixing occurred over only part of the core, $r \leq r_s$. The problem, here, is the apparent lack of universality (from an experimental

point of view) of this model.

Finally, another approach [133]-[134] has been to invoke the presence of a hyperviscosity, by introducing an extra diffusion-type term in Ohm's law. Numerical computations have established that fast crashes can be obtained in this manner, but the physical origin of the hyperviscosity has not been identified.

In conclusion, great progress has been made in understanding the basic physics of the sawtooth crash in toroidal experiments. Some possible explanations for the fast time scales in latest experiments are being developed, though no model is completely acceptable yet. The phenomenon of sawteeth is far richer than presented here: there exist compound sawteeth [6], [130]-[131], and a possible theoretical model for them has been presented in [135]. Similarly, there exists a vast literature on nonlinear evolution of $m^0 = 1$ modes, e.g., [136]-[141], which will require a separate review.

Acknowledgments

This work has been supported in part by the U.S. Department of Energy, under Contract DE-FG02-91ER-54109. The author wishes to thank B. Coppi, F. Pegoraro, F. Porcelli, and L. E. Zakharov for useful conversations.

REFERENCES

- [1] S. von Goeler, W. Stodiek, and N. Sauthoff, *Phys. Rev. Lett.* **33**, 1201 (1974).
- [2] M. N. Rosenbluth, R. Y. Dagazian, and P. H. Rutherford, *Phys. Fluids* **16**, 1894 (1973).
- [3] B. B. Kadomtsev, *Sov. J. Plasma Phys.* **1**, 389 (1975).
- [4] B. Coppi, R. Galvão, R. Pellat, M. N. Rosenbluth, and P. H. Rutherford, *Sov. J. Plasma Phys.* **2**, 533 (1976).
- [5] G. Ara, B. Basu, B. Coppi, G. Laval, M. N. Rosenbluth, and B. V. Waddell, *Ann. Phys. (NY)* **112**, 443 (1978).
- [6] D. J. Campbell, R. D. Gill, C. W. Gowers, J. A. Wesson, D. V. Bartlett, C. H. Best, S. Coda, A. E. Costley, A. Edwards, S. E. Kissel, R. M. Niestadt, R. W. Piekaar, R. Prentice, R. T. Ross, B. J. D. Tubbing, *Nucl. Fusion* **26**, 1085 (1986).
- [7] W. Pfeiffer, F. B. Marcus, C. J. Armentrout, G. L. Jahns, T. W. Petrie, and R. E. Stockdale, *Nucl. Fusion* **25**, 655 (1985).
- [8] A. W. Edwards, D. J. Campbell, W. W. Englehardt, H.-U. Fahrback, R. D. Gill, R. S. Granetz, S. Tsuji, B. J. D. Tubbing, A. Weller, J. Wesson, and D. Zasche, *Phys. Rev. Lett.* **57** 210 (1986).
- [9] Y. Nagayama, S. Tsuji, and K. Kawahata, *Phys. Rev. Lett.* **61**, 1839 (1988).
- [10] M. N. Bussac, R. Pellat, D. Edery, and J. L. Soulé, *Phys. Rev. Lett.* **35**, 1638 (1975).
- [11] E. Westerhof, P. Smeulders, and N. Lopes Cardozo, *Nucl. Fusion* **29**, 1056 (1989).
- [12] D. J. Campbell, J. G. Cordey, A. W. Edwards, R. D. Gill, E. Lazzaro, G. Magyar, A. L. McCarthy, J. O'Rourke, F. Pegoraro, F. Porcelli, P. Smeulders, D. F. H. Start,

- P. Stubberfield, J. A. Wesson, E. Westerhof, and D. Zasche, in *Plasma Physics and Controlled Nuclear Fusion Research 1988* (IAEA, Vienna, 1989), vol. 1, p. 377.
- [13] E. D. Fredrickson, K. M. McGuire, Y. Nagayama, M. Bell, A. Cavallo, P. Efthimion, H. Fleishmann, A. Janos, D. Johnson, D. Mansfield, D. A. Monticello, H. Park, W. Stodiek, G. Taylor, M. Ulrickson, P. V. Savrukhin, I. Semenov, R. N. Dexter, J. A. Goetz, E. J. Haines, M. A. LaPointe, S. C. Prager, J. C. Sprott, and I. H. Tan, in *Plasma Physics and Controlled Nuclear Fusion Research 1990* (IAEA, Vienna, 1991), vol. 1, p. 559.
- [14] Y. Nagayama, K. McGuire, A. Cavallo, E. Fredrickson, A. Janos, and G. Taylor, *Bull. Am. Phys. Soc.* **35**, 2087 (1990).
- [15] J. Wesson, A. W. Edwards, and R. S. Granetz, *Nucl. Fusion* **31**, 111 (1991).
- [16] M. Kaufmann, K. Behringer, G. Fussmann, O. Gruber, K. Lackner, R. S. Lang, V. Mertens, R. Nolte, W. Sandmann, K.-H. Steuer, G. Becker, H. Bessenrodt-Weberpals, B. Bomba, H.-S. Bosch, K. Brau, H. Bruhns, K. Büchl, R. Büsche, A. Carlson, G. Dodel, A. Eberhagen, H.-U. Fahrbach, O. Gehre, K. W. Gentle, J. Gernhardt, L. Giannone, G. Von Gierke, E. Glock, S. von Goeler, G. Haas, W. Heermann, J. Hofmann, E. Holzhauser, K. Hübner, G. Janeschitz, A. Kallenbach, O. Kardaun, F. Karger, O. Klüber, M. Kornherr, K. Kreiger, L. Lengyel, G. Lisitano, M. Lörcher, H. M. Mayer, K. McCormick, D. Meisel, E. R. Müller, H. D. Murmann, J. Neuhauser, H. Niedermeyer, J.-M. Noterdaeme, W. Poschenrieder, D. E. Roberts, H. Röhr, A. Rudyj, F. Rytter, F. Schneider, U. Schneider, E. Sevillano, G. Siller, E. Simnet, F. X. Söldner, E. Speth, A. Stäbler, U. Stroth, N. Tsois, O. Vollmer, F. Wagner, and H. Würtz, in

Plasma Physics and Controlled Nuclear Fusion Research 1988 (IAEA, Vienna, 1989),
vol. 1, p. 229.

- [17] Y. Kamada, R. Yoshino, M. Nagani, and T. Ozeki, *Nucl. Fusion* **31**, 23 (1991).
- [18] C. Janicki, R. Décoste, and C. Simm, *Phys. Rev. Lett.* **62**, 3038 (1989).
- [19] W. A. Newcomb, *Ann. Phys. (NY)* **10**, 232 (1967).
- [20] L. E. Zakharov, *Sov. J. Plasma Phys.* **4**, 503 (1978).
- [21] S. I. Braginskii, in **Reviews of Plasma Physics**, edited by M. A. Leontovich (Consultants Bureau, 1965), vol. 1, p. 214.
- [22] H. Soltwisch, W. Stodiek, J. Manickam, and J. Schlüter, in *Plasma Physics and Controlled Nuclear Fusion Research 1986* (IAEA, Vienna, 1987), vol. 1, p. 263.
- [23] M. Murakami, V. Arunasalam, J. D. Bell, M. G. Bell, M. Bitter, W. R. Blanchard, F. Boody, N. Bretz, R. Budny, C. E. Bush, J. D. Callen, J. L. Cecchi, S. Cohen, R. J. Colchin, S. K. Combs, J. Coonrod, S. L. Davis, D. Dimock, H. F. Dylla, P. C. Efthimion, L. C. Emerson, A.C. England, H. P. Eubank, R. Fonck, E. Fredrickson, H. P. Furth, L. R. Grisham, S. von Goeler, R. J. Goldston, B. Grek, R. Groebner, R. J. Hawryluk, H. Hendel, K. W. Hill, D. L. Hillis, W. Heidbrink, R. Hulse, D. Johnson, L. C. Johnson, R. Kaita, R. Kampenschroer, S. M. Kaye, S. Kilpatrick, H. Kugel, P. H. LaMarche, R. Little, C. H. Ma, D. Manos, D. Mansfield, M. McCarthy, R. T. McCann, D. C. McCune, K. McGuire, D. M. Meade, S. S. Medley, S. L. Milora, D. R. Mikkelsen, D. Mueller, E. Nieschmidt, D. K. Owens, V. K. Pare, H. Park, B. Prichard, A. Ramsey, D. A. Rasmussen, M. H. Redi, A. L. Roquemore, P. H. Rutherford, N. R. Sauthoff, J. Schivell, G. L. Schmidt, S. D. Scott, S. Sesnic, M. Shimada, J. E.

Simpkins, J. Sinnis, F. Stauffer, J. Strachan, B. Stratton, G. D. Tait, G. Taylor, C. E. Thomas, H. H. Towner, M. Ulrickson, R. Wieland, J. B. Wilgen, M. Williams, K.-L. Wong, S. Yoshikawa, K. M. Young, M. C. Zarnstorff, and S. Zweben, *Plasma Phys. Cont. Fusion* **28**, 17 (1986).

- [24] M. C. Zarnstorff, V. Arunasalam, C. W. Barnes, M. G. Bell, M. Bitter, H.-S. Bosch, N. L. Bretz, R. Budny, C. E. Bush, A. Cavallo, T. K. Chu, S. A. Cohen, P. L. Colestock, S. L. Davis, D. L. Dimock, H. F. Dylla, P. C. Efthimion, A. B. Ehrhardt, R. J. Fonck, E. D. Fredrickson, H. P. Furth, G. Gammel, R. J. Goldston, G. J. Greene, B. Grek, L. R. Grisham, G. W. Hammett, R. J. Hawryluk, H. W. Hendel, K. W. Hill, E. Hinnov, J. C. Hosea, R. B. Howell, H. Hsuan, R. A. Hulse, K. P. Jaehnig, A. C. Janos, D. L. Jassby, F. C. Jobes, D. W. Johnson, L. C. Johnson, R. Kaita, C. Kieras-Phillips, S. J. Kilpatrick, V. A. Krupin, P. H. LaMarche, B. LeBlanc, R. Little, A. I. Lysojvan, D. M. Manos, D. K. Mansfield, E. Mazzucato, R. T. McCann, M. P. McCarthy, D. C. McCune, K. M. McGuire, D. H. McNeill, D. M. Meade, S. S. Medley, D.R. Mikkelsen, R. W. Motley, D. Mueller, Y. Murakami, J. A. Murphy, E. B. Nieschmidt, D. K. Owens, H. K. Park, A. T. Ramsey, M. H. Redi, A. L. Roquemore, P. H. Rutherford, T. Saito, N. R. Sauthoff, G. Schilling, J. Schivell, G. L. Schmidt, S. D. Scott, J. C. Sinnis, J. E. Stevens, W. Stodiek, J. D. Strachan, B. C. Stratton, G. D. Tait, G. Taylor, J. R. Timberlake, H. H. Towner, M. Ulrickson, S. von Goeler, R. M. Wieland, M. D. Williams, J. R. Wilson, K.-L. Wong, S. Yoshikawa, K. M. Young, and S. J. Zweben, in *Plasma Physics and Controlled Nuclear Fusion Research 1988* (IAEA, Vienna, 1989), vol. 1, p. 183.

- [25] D. V. Bartlett, R. J. Bickerton, M. Brusati, D. J. Campbell, J. P. Christiansen, J. G. Cordey, S. Corti, A. E. Costley, A. Edwards, J. Fessey, M. Gadeberg, A. Gibson, R. D. Gill, N. Gottardi, A. Gondhalekar, C.W. Gowers, F. Hendriks, O. N. Jarvis, E. Källne, J. Källne, S. Kissel, L. C. J. M. De Kock, H. Krause, E. Lazzaro, P. J. Lomas, F. K. Mast, P. D. Morgan, P. Nielsen, R. Prentice, R. T. Ross, J. O'Rourke, G. Sadler, F. C. Schüller, M. F. Stamp, P. E. Stott, D. R. Summers, A. Tanga, A. Taroni, P. R. Thomas, F. Tibone, G. Tonetti, B. J. D. Tubbing, and M. L. Watkins, *Nucl. Fusion* **28**, 73 (1988).
- [26] V. P. Bhatnagar, A. Taroni, J. J. Ellis, J. Jacquinet, and D. F. H. Start, *Plasma Phys. Cont. Fusion* **31**, 2111 (1989).
- [27] M. J. Lighthill, **An Introduction to Fourier Analysis and Generalized Functions** (Univ. of Cambridge, Cambridge, 1958).
- [28] F. Pegoraro and T. J. Schep, *Plasma Phys. Cont. Fusion* **28**, 647 (1986).
- [29] B. Coppi, J. Greene, and J. Johnson, *Nucl. Fusion* **6**, 101 (1966).
- [30] I. M. Gelf'and and G. E. Shilov, **Generalized Functions** (Academic, NY, 1964).
- [31] L. J. Slater, in **Handbook of Mathematical Functions**, edited by M. Abramowitz and I. A. Stegun (Dover, NY, 1972), p. 503.
- [32] M. N. Bussac, R. Pellat, D. Edery, and J. L. Soulé, in *Plasma Physics and Controlled Nuclear Fusion Research 1976* (IAEA, Vienna, 1977), vol. 1, p. 607.
- [33] B. Coppi, R. Englade, S. Migliuolo, F. Porcelli, and L. Sugiyama, in *Plasma Physics and Controlled Nuclear Fusion Research 1986* (IAEA, Vienna, 1987), vol. 3, p. 397.
- [34] F. Porcelli, PhD Thesis, Scuola Normale Superiore (Pisa, Italy, 1987).

- [35] S. Migliuolo, F. Pegoraro, and F. Porcelli *Phys. Fluids* **B3**, 1338 (1991).
- [36] P. H. Rutherford, and H. P. Furth, Princeton Plasma Physics Laboratory report MATT-872 (unpublished, 1971).
- [37] F. Porcelli, *Phys. Fluids* **30**, 1734 (1987).
- [38] B. Coppi and M. N. Rosenbluth, in *Plasma Physics and Controlled Nuclear Fusion Research 1965* (IAEA, Vienna, 1966), vol. 1, p. 617.
- [39] F. Porcelli and S. Migliuolo, *Phys. Fluids* **29**, 1741 (1986).
- [40] F. Porcelli, *Phys. Rev. Lett.* **66**, 425 (1991).
- [41] J. F. Drake and R. G. Kleva, *Phys. Rev. Lett.* **66**, 1458 (1991).
- [42] B. Basu and B. Coppi, *Phys. Fluids* **24**, 465 (1981).
- [43] J. F. Drake, *Phys. Fluids* **21**, 1777 (1978).
- [44] F. Pegoraro, F. Porcelli, and T. J. Schep, *Phys. Fluids* **B1**, 364 (1989).
- [45] R. G. Kleva, *Phys. Fluids* **B3**, 102 (1991).
- [46] J. A. Wesson, *Nucl. Fusion* **30**, 2545 (1990).
- [47] N. A. Krall and A. W. Trievelpiece, **Principles of Plasma Physics** (McGraw-Hill, NY, 1973).
- [48] J. F. Drake, Y. C. Lee, Liu Chen, P. H. Rutherford, P. K. Kaw, J. Y. Hsu, and C. S. Liu, *Nucl. Fusion* **18**, 1583 (1978).
- [49] T. M. Antonsen, jr., and B. Coppi, *Phys. Lett.* **A81**, 335 (1981).
- [50] G. B. Crew, T. M. Antonsen, jr., and B. Coppi, *Nucl. Fusion* **22**, 41 (1982).
- [51] G. B. Crew and J. J. Ramos, *Nucl. Fusion* **26**, 1475 (1986).
- [52] B. Coppi, J. W. K. Mark, L. Sugiyama, and G. Bertin, *Ann. Phys. (NY)* **119**, 379

(1979).

- [53] S. Migliuolo, *Nucl. Fusion* **31**, 365 (1991).
- [54] H. L. Berk, S. M. Mahajan, and Y. Z. Zhang, *Phys. Fluids* **B3**, 351 (1991).
- [55] N. C. Christofilos in *Proceedings of the Second UN General Conference on the Peaceful Uses of Atomic Energy* (UN, Geneva, 1958), vol. 32, p. 279.
- [56] R. N. Sudan and E. Ott, *Phys. Rev. Lett.* **38**, 355 (1974).
- [57] R. A. Dandl, H. O. Eason, G. E. Guest, C. L. Hedrick, H. Ikegami, and D. B. Nelson, in *Plasma Physics and Controlled Nuclear Fusion Research 1974* (IAEA, Vienna, 1975), vol. 2, p. 141.
- [58] M. N. Rosenbluth, S. T. Tsai, J. W. VanDam, and M. G. Engquist, *Phys. Rev. Lett.* **51**, 1967 (1983).
- [59] G. Bateman, **MHD Instabilities** (MIT Press, Cambridge, 1978).
- [60] J. Jacquinet, *Bull. Am. Phys. Soc.* **32**, 1713 (1987).
- [61] D. J. Campbell, D. F. H. Start, J. A. Wesson, D. V. Bartlett, V. P. Bhatnagar, M. Bures, J. G. Cordey, G. A. Cottrell, P. A. Dupperex, A. W. Edwards, C. D. Challis, C. Gormezano, C. W. Gowers, R. S. Granetz, J. H. Hamnen, T. Hellsten, J. Jacquinet, E. Lazzaro, P. J. Lomas, N. Lopes Cardozo, P. Mantica, J. A. Snipes, D. Stork, P. E. Stott, P. R. Thomas, E. Thompson, K. Thomser, and G. Tonetti, *Phys. Rev. Lett.* **60**, 2148 (1988).
- [62] D. J. Campbell and the JET Team, in *Plasma Physics and Controlled Nuclear Fusion Research 1990* (IAEA, Vienna, 1991), vol. 1, p. 437.
- [63] A. M. Messiaen, H. Conrads, M. Gaigneaux, J. Ongena, R. Weynants, G. Betschinger,

- J. M. Beuken, P. Cornelissen, T. Delvigne, F. Durodie, H. G. Esser, H. Euringer, G. Fuchs, B. Giesen, B. Görg, D. L. Hillis, F. Hoenen, P. Hütteman, M. Jadoul, R. Koch, H. Kever, M. Korten, W. Kohlhaas, D. Lebeau, M. Lochter, D. Reiter, D. Rusbüldt, M. Sauer, J. Schlueter, H. Soltwisch, M. Storch, G. Telesa, R. Uhlemann, P. E. Vandenplas, R. Van Nieuwenhove, G. Van Oost, G. Van Wassenhove, G. Waidmann, J. G. Wang, J. Winter, G. H. Wolf, and J. W. Yang, *Plasma Phys. Cont. Fus.* **32**, 889 (1990).
- [64] D. Meade and the TFTR Group, in *Plasma Physics and Controlled Nuclear Fusion Research 1990* (IAEA, Vienna, 1991), vol. 1, p. 9.
- [65] B. B. Kadomtsev, F. S. Troyon, M. L. Watkins, P. H. Rutherford, M. Yoshikawa, and V. S. Mukhovatov, *Nucl. Fusion* **30**, 1675 (1990).
- [66] F. X. Söldner, K. McCormick, D. Eckhartt, M. Kornherr, F. Leuterer, R. Bartiromo, G. Becker, H. S. Bosch, H. Brocken, H. Derfler, A. Eberhagen, G. Fussmann, O. Gehre, J. Gernhardt, G. von Gierke, A. Giuliana, E. Glock, O. Gruber, G. Haas, M. Hesse, J. Hofmann, A. Izvozhikov, G. Janeschitz, F. Karger, M. Keilhacker, O. Klüber, K. Lackner, M. Lenoli, G. Lisitano, F. Mast, H. M. Mayer, D. Meisel, V. Mertens, E. R. Müller, M. München, H. Murmann, H. Niedermeyer, A. Pietrzyk, W. Poschenrieder, H. Rapp, H. Riedler, H. Röhr, F. Ryter, K. H. Schmitter, F. Schneider, C. Setzensack, G. Siller, P. Smeulders, E. Speth, K. H. Steuer, T. Vien, O. Vollmer, F. Wagner, F. von Woyna, and D. Zasche, *Phys. Rev. Lett.* **57**, 1137 (1986).
- [67] B. N. Kuvshinov and P. V. Savrukhin, *Sov. J. Plasma Phys.* **16**, 353 (1990).
- [68] M. Nagami and the JT-60 Team, in *Plasma Physics and Controlled Nuclear Fusion*

Research 1990 (IAEA, Vienna, 1991), vol 1, p. 53.

- [69] D. Johnson, M. Bell, M. Bitter, K. Bol, K. Brau, D. Buchenauer, R. Budny, T. Crowley, S. Davis, F. Dylla, H. Eubank, H. Fishman, R. Fonck, R. Goldston, B. Grek, R. Grimm, R. Hawryluk, H. Hsuan, R. Kaita, S. Kaye, H. Kugel, J. Manickam, D. Manos, D. Mansfield, D. Marty, E. Mazzucato, R. McCann, D. McCune, K. McGuire, R. Motley, D. Mueller, K. Oasa, J. Olivain, M. Okabayashi, K. Owens, J. Ramette, C. Reverdin, M. Reusch, N. Sauthoff, G. Schilling, G. Schmidt, S. Sesnic, R. Slusher, J. Strachan, S. Suckerwer, C. Surko, H. Takahashi, F. Tenney, P. Thomas, H. Towner, and J. Valley, in *Plasma Physics and Controlled Nuclear Fusion Research 1982* (IAEA, Vienna, 1983), vol. 1, p. 9.
- [70] K. McGuire, R. Goldston, M. Bell, M. Bitter, K. Bol, K. Brau, D. Buchenauer, T. Crowley, S. Davis, F. Dylla, H. Eubank, H. Fishman, R. Fonck, B. Grek, R. Grimm, R. Hawryluk, H. Hsuan, R. Hulse, R. Izzo, R. Kaita, S. Kaye, H. Kugel, D. Johnson, J. Manickam, D. Manos, D. Mansfield, E. Mazzucato, R. McCann, D. McCune, D. Monticello, R. Motley, D. Mueller, K. Oasa, M. Okabayashi, K. Ownes, W. Park, M. Reusch, N. Sauthoff, G. Schmidt, S. Sesnic, R. Slusher, J. Strachan, C. Surko, H. Takahashi, F. Tenney, P. Thomas, H. Towner, J. Valley, and R. B. White, *Phys. Rev. Lett.* **50**, 891 (1983).
- [71] J. D. Strachan, B. Grek, W. Heidbrink, D. Johnson, S. M. Kaye, H. W. Kugel, B. LeBlanc, and K. McGuire, *Nucl. Fusion* **25**, 853 (1985).
- [72] D. O. Overskei, C. J. Armentrout, J. F. Baur, F. P. Blau, G. Bramson, K. H. Burrell, R. P. Chase, J. C. DeBoo, S. Ejima, E. S. Fairbanks, R. Groebner, C. L. Hsieh, G. L.

- Jahns, C. L. Kahn, D. H. Kellman, D. Knowles, J. Lieber, J. M. Lohr, N. Ohyaabu, T. W. Petrie, L. C. Rottler, D. P. Schissel, R. P. Seraydarian, J. R. Smith, R. T. Snider, R. D. Staumbaugh, R. E. Stockdale, H. St. John, E. J. Strait, C. S. Tucker, D. Vaslow, S. S. Wojtowicz, S. K. Wong, and the Doublet III Operations, Neutral Beam, and Theory Groups, in *Heating in Toroidal Plasmas 1984*, edited by H. Knoepfel and E. Sindoni (ENEA, Rome, 1984), vol. 1, p. 21.
- [73] W. W. Heidbrink, *Nucl. Fusion* **30**, 1015 (1990).
- [74] W. W. Heidbrink, K. Bol, D. Buchenauer, R. Fonck, G. Gammel, K. Ida, R. Kaita, S. Kaye, H. Kugel, B. LeBlanc, W. Morris, M. Okabayashi, E. Powell, S. Sesnic, and H. Takahashi, *Phys. Rev. Lett.* **57**, 835 (1986).
- [75] A. W. Morris, E. D. Fredrickson, K. M. McGuire, M. G. Bell, M. S. Chance, R. J. Goldston, R. Kaita, J. Manickam, S. S. Medley, N. Pomphrey, S. D. Scott, and M. C. Zarnstorff, in *Proceedings of the 14th European Conference on Controlled Fusion and Plasma Heating*, Madrid (EPS, Geneva, 1987), vol. 11D, part I, p. 189.
- [76] M. F. F. Nave, D. J. Campbell, E. Joffrin, F. B. Marcus, G. Sadler, P. Smeulders, and K. Thomsen, *Nucl. Fusion* **31**, 697 (1991).
- [77] J. F. Drake, T. M. Antonsen, jr., A. B. Hassam, and N. T. Gladd, *Phys. Fluids* **26**, 2509 (1983).
- [78] B. Coppi, M. N. Rosenbluth, and R. N. Sudan, *Ann. Phys. (NY)* **55**, 207 (1969).
- [79] B. Coppi, S. Migliuolo, and F. Porcelli, *Phys. Fluids* **31**, 1630 (1988).
- [80] P. H. Rutherford and E. A. Frieman, *Phys. Fluids* **11**, 569 (1968).
- [81] T. M. Antonsen, jr., and B. Lane, *Phys. Fluids* **23**, 1205 (1980).

- [82] R. Betti and J. P. Freidberg *Phys. Fluids* **B3**, 538 (1991).
- [83] B. Coppi, *Riv. Nuovo Cimento* **1**, 357 (1969).
- [84] B. Coppi and G. Rewoldt, in *Advances in Plasma Physics*, edited by A. Simon and W. B. Thompson (Interscience, NY, 1976), vol. 6, p. 421.
- [85] G. Rewoldt, W. M. Tang, and M. S. Chance, *Phys. Fluids* **25**, 480 (1982).
- [86] B. Coppi, S. Migliuolo, and Y.-K. Pu, *Phys. Fluids* **B2**, 2333 (1990).
- [87] F. Porcelli, H. L. Berk, and Y. Z. Zhang, *Phys. Fluids* (submitted, 1991).
- [88] B. Coppi, S. Migliuolo, F. Pegoraro, and F. Porcelli, *Phys. Fluids* **B2**, 927 (1990).
- [89] F. Porcelli, *Plasma Phys. and Cont. Fusion* (in press, 1991).
- [90] B. Coppi and the Ignitor Group, in *Plasma Physics and Controlled Nuclear Fusion Research 1988* (IAEA, Vienna, 1989), vol. 3, p. 357.
- [91] P. J. Davis, in *Handbook of Mathematical Functions*, edited by M. Abramowitz and I. A. Stegun (Dover, NY, 1972), p. 253.
- [92] B. Coppi, R. J. Hastie, S. Migliuolo, F. Pegoraro, and F. Porcelli, *Phys. Lett.* **A132**, 267 (1988).
- [93] B. Coppi, P. Detragiache, S. Migliuolo, F. Pegoraro, and F. Porcelli, *Phys. Rev. Lett.* **63**, 2733 (1989).
- [94] R. B. White, P. H. Rutherford, P. Colestock, and M. N. Bussac, *Phys. Rev. Lett.* **60**, 2038 (1988).
- [95] R. B. White, M. N. Bussac, and F. Romanelli, *Phys. Rev. Lett.* **62**, 539 (1989).
- [96] Y. Z. Zhang, H. L. Berk, and S. M. Mahajan, *Nucl. Fusion* **29**, 848 (1989).
- [97] Y. Z. Zhang and H. L. Berk, *Phys. Lett.* **A143**, 250 (1990).

- [98] Liu Chen, R. B. White, and M. N. Rosenbluth, *Phys. Rev. Lett.* **52**, 1122 (1984).
- [99] Y.-P. Chen, R. J. Hastie, F.-J. Ke, S.-D. Cai, and Liu Chen, *Acta Phys. Sin.* **37**, 546 (1988).
- [100] C. Z. Cheng, *Phys. Fluids* **B2**, 1495 (1990).
- [101] F. Porcelli, D. J. Campbell, W. D. Diachenko, L.-G. Eriksson, J. Jacquinet, L. S. Levin, D. F. H. Start, and A. Taroni, in *Proceedings of the 17th European Conference on Controlled Fusion and Plasma Heating*, Amsterdam (EPS, Geneva, 1990), vol. 14B, part I, p. 327.
- [102] B. N. Kuvshinov and A. B. Mikhailovskii, *Sov. J. Plasma Phys.* **13**, 527 (1987).
- [103] F. Pegoraro, F. Porcelli, and T. J. Schep, *Phys. Fluids* **B3**, 1319 (1991).
- [104] C. Litwin, *Phys. Rev. Lett.* **60**, 2375 (1988).
- [105] D. J. Campbell, L. Baylor, V. P. Bhatnagar, M. Bures, A. Cheetham, J. G. Cordey, G. A. Cottrell, J. de Haas, A. W. Edwards, L. G. Eriksson, A. Gondhalekar, N. Gottardi, R. J. Hastie, T. Hellsten, J. Jacquinet, E. Lazzaro, L. McCarthy, P. D. Morgan, J. O'Rourke, D. Pearson, F. Pegoraro, F. Porcelli, G. L. Schmidt, J. A. Snipes, D. F. H. Start, P. Stubberfield, P. R. Thomas, K. Thomsen, B. J. D. Tubbing, and J. A. Wesson, in *Proceedings of the 15th European Conference on Controlled Fusion and Plasma Heating*, Dubrovnik (EPS, Geneva, 1988), vol. 12B, part I, p. 377.
- [106] C. Litwin, *Phys. Fluids* **B2**, 463 (1990).
- [107] B. Coppi and F. Porcelli, *Phys. Rev. Lett.* **57**, 2272 (1986).
- [108] R. B. White, Liu Chen, F. Romanelli, and R. Hay, *Phys. Fluids* **28**, 278 (1985).
- [109] H. Biglari and Liu Chen, *Phys. Fluids* **29**, 1760 (1986).

- [110] B. Coppi and F. Porcelli, *Fusion Technology* **14**, 447 (1988).
- [111] W. W. Heidbrink, K. Bol, D. Buchenauer, R. Fonck, G. Gammel, K. Ida, R. Kaita, S. Kaye, H. Kugel, B. LeBlanc, W. Morris, M. Okabayashi, E. Powell, S. Sesnic, and H. Takahashi, *Phys. Rev. Lett.* **57**, 835 (1986).
- [112] R. Kaita, K. Bol, P. Couture, R. Fonck, G. Gammel, W. Heidbrink, K. Ida, G. Jahns, S. Kaye, H. Kugel, B. Leblanc, W. Morris, G. Navratil, N. Ohyabu, M. Okabayashi, S. Paul, M. Reusch, S. Sesnic, and H. Takahashi, *Plasma Phys. Cont. Fusion* **28**, 1319 (1986).
- [113] W. W. Heidbrink, and G. Sager, *Nucl. Fusion* **30**, 1015 (1990).
- [114] F. Romanelli and Liu Chen, *Phys. Fluids* **B3**, 329 (1991).
- [115] G. L. Jahns, M. Soler, B. V. Waddell, J. D. Callen, and H. R. Hicks, *Nucl. Fusion* **18**, 609 (1978).
- [116] W. P. West, D. M. Thomas, J. S. deGrassie, and S. B. Zheng, *Phys. Rev. Lett.* **58**, 2758 (1987).
- [117] A. Gibson and the JET Team, *Plasma Phys. Cont. Fusion* **30**, 1375 (1988).
- [118] R. D. Gill, A. W. Edwards, and A. Weller, *Nucl. Fusion* **29**, 821 (1989).
- [119] D. Wróbleski, L. K. Huang, H. W. Moos, and P. E. Phillips, *Phys. Rev. Lett.* **61**, 1724 (1988).
- [120] J. A. Wesson, *Plasma Phys. Cont. Fusion* **28**, 243 (1986).
- [121] J. J. Ramos, *Phys. Rev. Lett.* **60**, 523 (1988).
- [122] A.Y Aydemir and R. D. Hazeltine, *Phys. Rev. Lett.* **59**, 649 (1987).
- [123] U. Stroth, G. Fussmann, K. Krieger, V. Mertens, F. Wagner, M. Bessenrodt Weber-

pals, R. BÜchse, L. Giannone, H. Herrmann, G. Simnet, and K. H. Steuer, Max Planck Institut für Plasmaphysik preprint IPP III/178 (1991).

- [124] J. O'Rourke, *Plasma Phys. Cont. Fusion* **33**, 289 (1991).
- [125] F. M. Levinton, R. J. Fonck, G. M. Gammel, R. Kaita, H. W. Kugel, E. T. Powell, and D. W. Roberts, *Phys. Rev. Lett.* **60**, 2060 (1989).
- [126] R. G. Kleva, J. F. Drake, and R. E. Denton, *Phys. Fluids* **30**, 2119 (1987).
- [127] V. V. Parail and G. V. Pereverzev, *Sov. J. Plasma Phys.* **6**, 14 (1980).
- [128] Avinash, R. J. Hastie, J. B. Taylor, and S. C. Cowley, *Phys. Rev. Lett.* **59**, 2647 (1985).
- [129] V. V. Parail and G. V. Pereverzev, *Sov. J. Plasma Phys.* **6**, 14 (1980).
- [130] W. Pfeiffer, *Nucl. Fusion* **25**, 673 (1985).
- [131] S. B. Kim, *Nucl. Fusion* **26**, 1251 (1986).
- [132] W. Pfeiffer, F. B. Marcus, J. Armentrout, G. L. Jahns, T. W. Petrie, and R. E. Stockdale, *Nucl. Fusion* **25**, 655 (1985).
- [133] D. J. Ward and S. C. Jardin, *Nucl. Fusion* **29**, 905 (1989).
- [134] A. Y. Aydemir, *Phys. Fluids* **B2**, 2135 (1990).
- [135] R. E. Denton, J. F. Drake, R. G. Kleva, and D. A. Boyd, *Phys. Rev. Lett.* **23**, 2477 (1986).
- [136] B. V. Waddell, M. N. Rosenbluth, D. A. Monticello, and R. B. White, *Nucl. Fusion* **16**, 528 (1976).
- [137] M. N. Rosenbluth, D. A. Monticello, H. R. Strauss, and R. B. White, *Phys. Fluids* **19**, 1987 (1976).

- [138] D. Biskamp, *Phys. Rev. Lett.* **46**, 1522 (1981).
- [139] W. Park, D. A. Monticello, and R. B. White, *Phys. Fluids* **27**, 134 (1984).
- [140] R. D. Hazeltine, J. D. Meiss, and P. J. Morrison, *Phys. Fluids* **29**, 163 (1986).
- [141] R. E. Denton, J. F. Drake, and R. G. Kleva, *Phys. Fluids* **30**, 1448 (1987).

Table I

Selected dimensionless quantities for various experiments

(OH = Ohmic, NB = neutral beams, ICRH = ion cyclotron, SUP = superset)

Experiment [ref.]	$\frac{r_s}{\bar{a}}$ (a)	q_0 (a)	$\frac{\nu_{ei}}{\bar{\omega}_{*e}}$	$\frac{k_{ 0} V_{Te}}{\nu_{ei}}$ (b)	$\frac{\rho_i}{\Delta_0}$ (b)
TEXTOR [22]	0.5	0.6	11.6	0.40	1.06
TFTR-OH [23]	0.3	(3/4)	6.0	0.35	1.06
TFTR-NB [23]	0.3	(3/4)	2.2	0.66	1.74
TFTR-SUP [24]	(1/3)	(3/4)	4.2	2.39	4.57
TFTR-SUP [24]	(1/2)	(3/4)	1.4	1.26	2.49
JET-OH [25]	0.3	(3/4)	5.7	0.32	1.09
JET-ICRH [26]	(1/3)	(3/4)	5.8	0.81	2.15
JET-ICRH [26]	(1/2)	(3/4)	3.3	0.35	0.98

(a) A parabolic q -profile is assumed within $r \leq r_s$. Values shown in parentheses are assumed (unknown experimentally); $\bar{a} \equiv$ mean minor radius.

(b) $k_{||0} \equiv k_{||}(x = \epsilon_\eta^{1/3})$ and $\Delta_0 \equiv \epsilon_\eta^{1/3} r_s / s(r_s)$ are chosen for purpose of illustration.

Table II

Selected Time Scales for Linear Growth of $M^0 = 1$ Modes

(OH = Ohmic, NB = neutral beam, ICRH = ion cyclotron, SUP = supershot)

Experiment * [ref.]	Resistive $\tau = \frac{1}{\epsilon_{\eta}^{1/3} \omega_A}$	Modified Res. $\tau = \frac{ \omega_{di} \hat{\omega}_{*e} }{\epsilon_{\eta} \omega_A^3}$	Collisionless ^(a) $\tau = \frac{r_s}{d \omega_A}$	FLR Coll. ^(b)
TEXTOR [22]	79 μ sec	n/a	158 μ sec	∞
TFTR-OH [23]	165 μ sec	n/a	146 μ sec	4 msec
TFTR-NB [23]	187 μ sec	692 μ sec	146 μ sec	3 msec
TFTR-SUP [24]	264 μ sec	25 msec	165 μ sec	∞
JET-OH [25]	228 μ sec	262 μ sec	242 μ sec	3 msec
JET-ICRH [26]	340 μ sec	10 msec	319 μ sec	∞

* Unless experimentally known, r_s/\bar{a} is set equal to 1/3.

^(a) $d \equiv c/\omega_{pe}$; this expression for τ is valid only for $\omega_{di} = \hat{\omega}_{*e} \rightarrow 0$

^(b) $\tau \equiv 1/\gamma$ is obtained from Ref. [40], by solving $(\gamma + i\omega_{di})(\gamma + i\hat{\omega}_{*e}) = \omega_A^2 (d\rho_i^2)^{4/3}/r_s^2$.

Figures

Fig. 1 Stability domain for resistive internal kink modes in fluid regimes, in the $\Omega_* - \hat{\lambda}_H$ plane. Here $\Omega_* \equiv \hat{\omega}_{*e}/\epsilon_\eta^{1/3}\omega_A$, $\hat{\lambda}_H \equiv \lambda_H/\epsilon_\eta^{1/3}$ and the stable regime for a given value of $1/\tau \equiv -\omega_{di}/\hat{\omega}_{*e}$ is above the corresponding curve.

Fig. 2 Normalized growth rate, $\gamma/\epsilon_\eta^{1/3}\omega_A$, of the resistive $m^0 = 1$ mode in the large ion Larmor radius regime (cf. Eq. (28) of Ref. [44]), in the negative λ_H regime. We take $\omega_{di} = -\hat{\omega}_{*e} = \omega_A(\rho_i/2r_s)$, setting temperature gradients to zero. Note the non-monotonic behavior of the curve for $\Omega_* \equiv \hat{\omega}_{*e}/\epsilon_\eta^{1/3}\omega_A = 3$, indicating connection of the resistive internal kink to the drift-tearing mode.

Fig. 3 Normalized mode frequency, $Re(\omega)/\epsilon_\eta^{1/3}\omega_A$, corresponding to the growth rates of the previous figure (large ion Larmor radius regime).

Fig. 4 Energetic particle functional, $\Lambda_k \equiv (s/\epsilon_s\beta_{ph})\lambda_k$, as function of $\omega/\bar{\omega}_{Dh}$, for high energy ICRH experiments in JET (cf. Ref. [101]). Here $\epsilon_s = r_s/R$, $s = rdq/dr|_{r_s}$, $\bar{\omega}_{Dh} = 1.2\mathcal{E}_h(1+2s)/(m_h\Omega_h Rr_s)$ and \mathcal{E}_h is the maximum energy of the trapped ions produced by ICRH.

Fig. 5 Energetic particle functional, $\Lambda_k \equiv (s/\epsilon_s^{3/2}\beta_{p\alpha})\lambda_k$, as a function of $\omega/\bar{\omega}_{D\alpha}$, for α -particles produced, with birth energy \mathcal{E}_α , in Ignitor (cf. Ref. [88]). Here $\epsilon_s = r_s/R$, $s = rdq/dr|_{r_s}$ and $\bar{\omega}_{D\alpha} \equiv \mathcal{E}_\alpha/(m_\alpha\Omega_\alpha Rr_s)$.

Fig. 6 Marginal stability curve in the $(\Delta\beta_p^2 = \beta_p^2 - \beta_{pc}^2, \beta_{p\alpha})$ plane, where β_{pc} is the critical value given, e.g. in Ref. [10]; β_p and $\beta_{p\alpha}$ are defined in Eq. (IV.33). Other

parameters are $\bar{\omega}_{D\alpha}/\omega_A = \sqrt{3}\mathcal{E}_\alpha/(m_\alpha\Omega_\alpha Rr_s V_A) = 0.2$ and $\omega_{di}/\omega_A = 0.05$, while the magnetic shear at the $q = 1$ surface is set at 0.6.

Fig. 7 Marginal stability curve and instability regimes for the case of an isotropic population of fusion α -particles in a high temperature ($\epsilon_\eta = 0$) plasma with $\omega_{di}/\bar{\omega}_{D\alpha} =$

0.1. Definition: $\hat{\beta}_{p\alpha} \equiv (r_s/R)^{3/2} [\beta_{p\alpha}/s(r_s)] (\omega_A/\bar{\omega}_{D\alpha})$

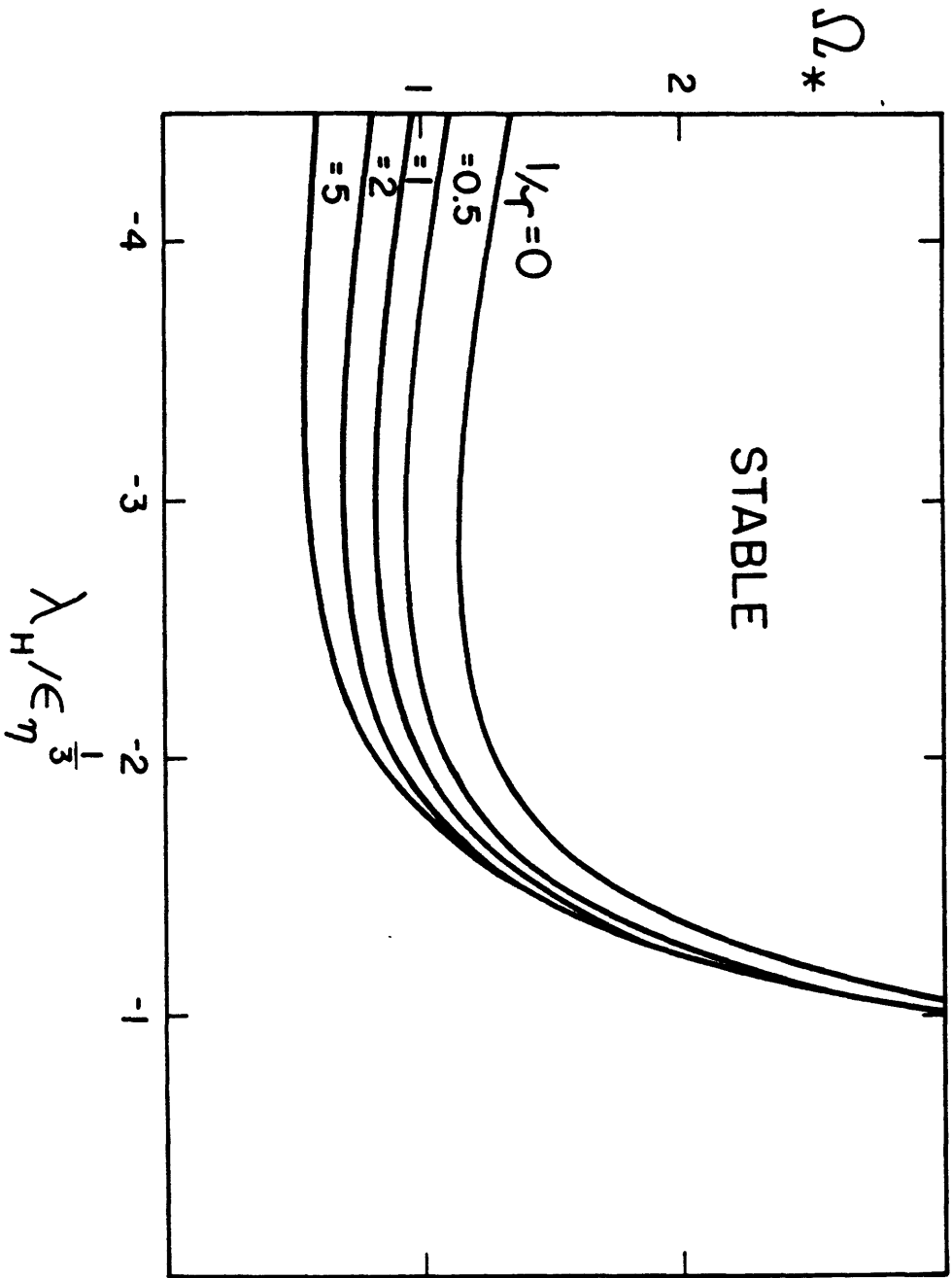


Fig. 1

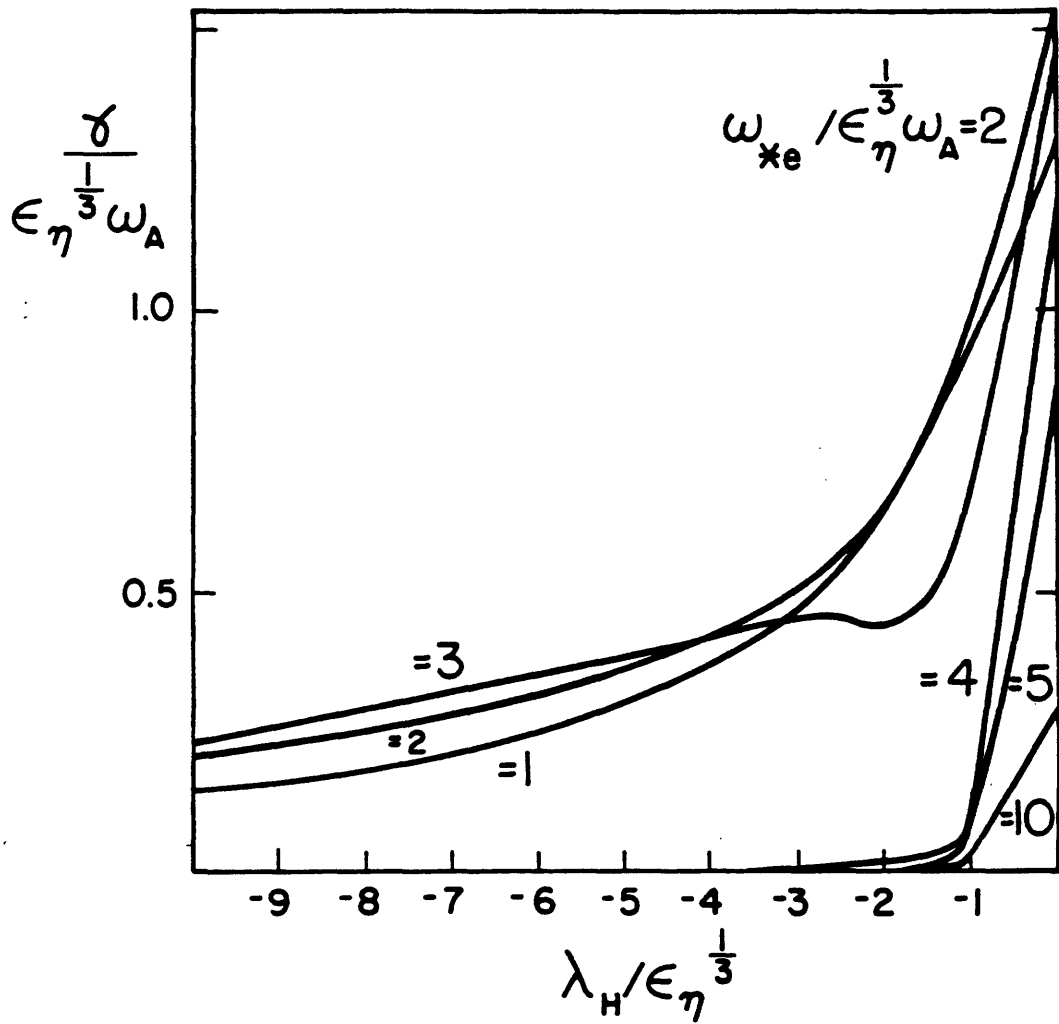


Fig. 2

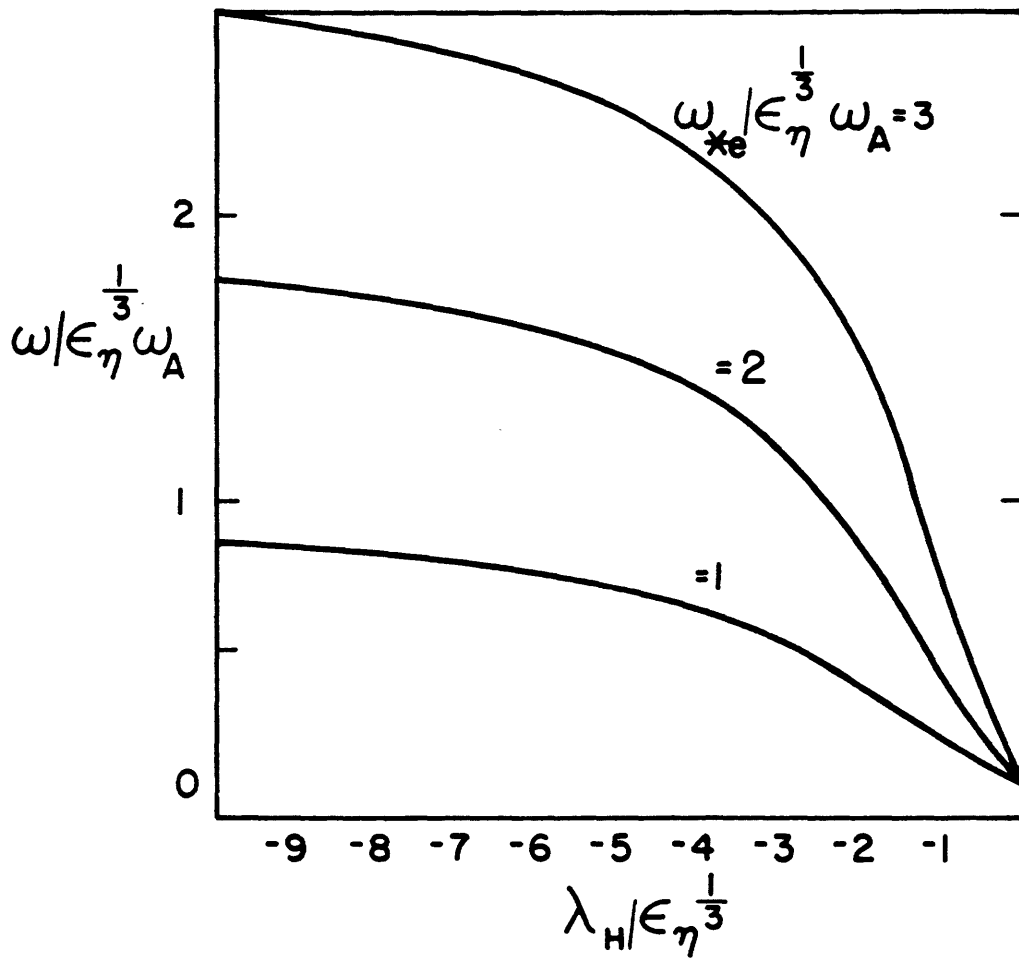


Fig. 3

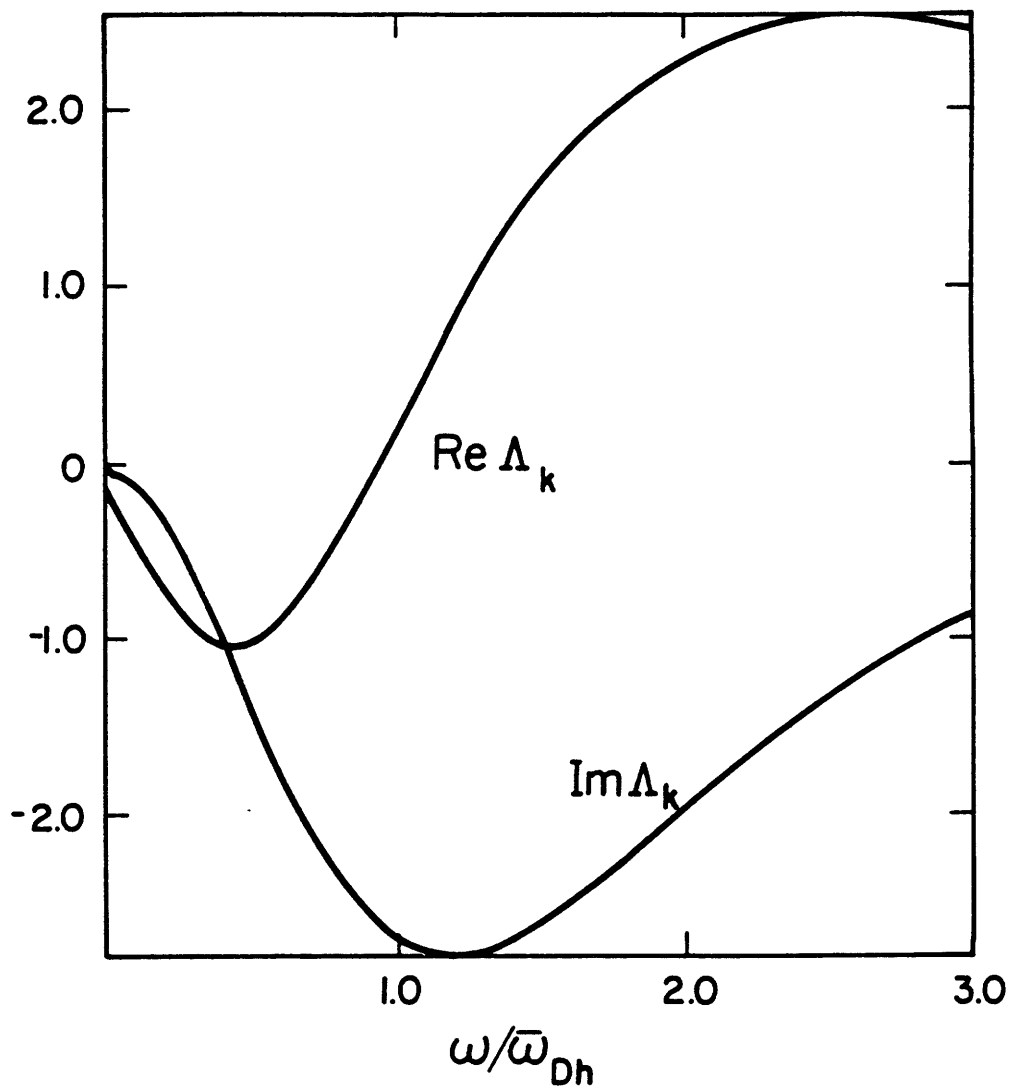


Fig. 4

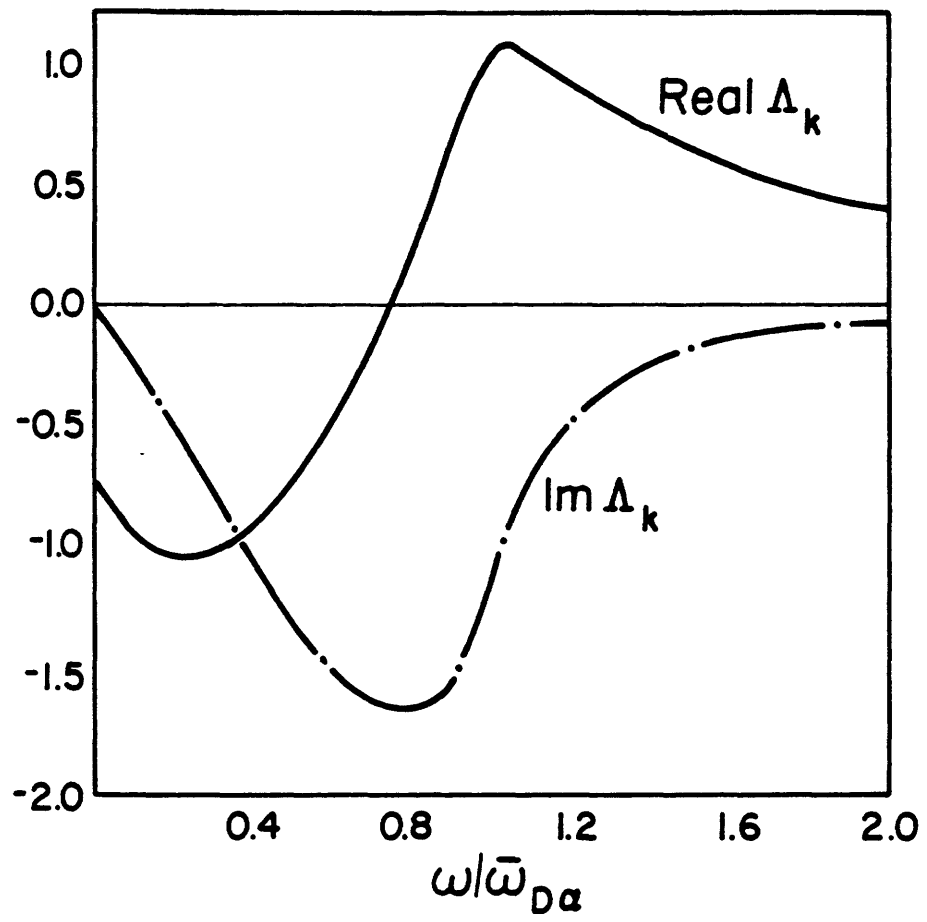


Fig. 5

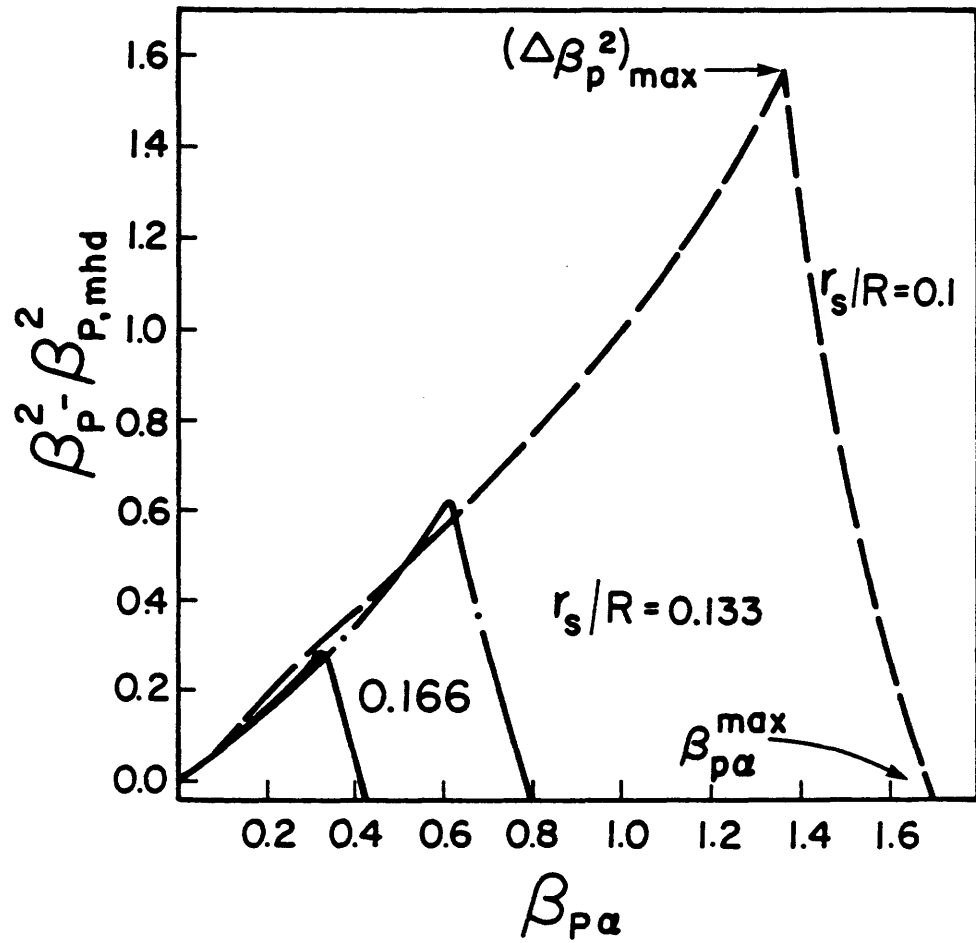


Fig. 6

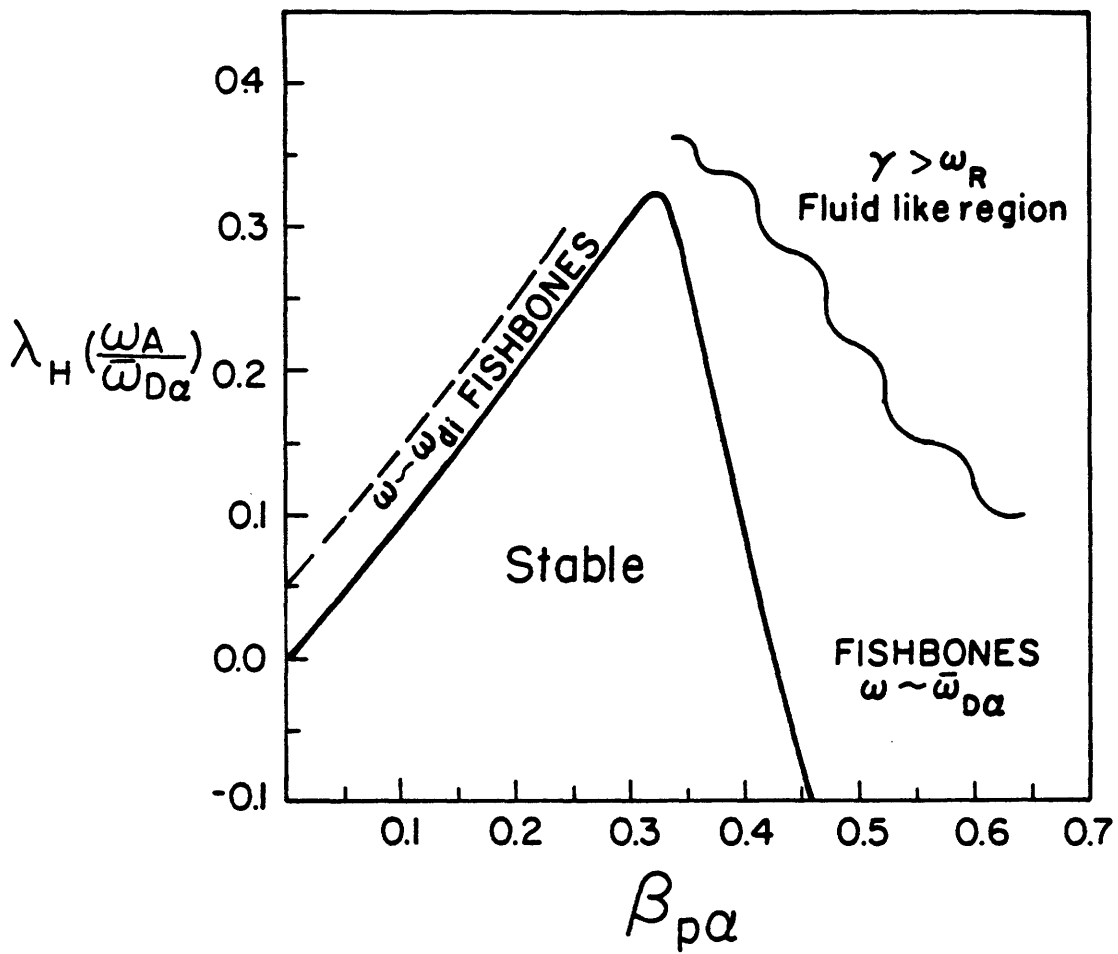


Fig. 7
